A REVISED DESIGN CONCEPT FOR
THE A-7E APPROACH POWER COMPENSATOR SYSTEM

David Haley Finney

NAVAL POSTGRADUATE SCHOOL
Monterey, California

THESIS

A REVISED DESIGN CONCEPT

FOR

THE A-7E APPROACH POWER COMPENSATOR SYSTEM

by

DAVID HALEY FINNEY

Thesis Advisor: Ronald A. Hess

March 1973

A Revised Design Concept

for

the A-7E Approach Power Compensator System

by

David Haley Finney
Lieutenant, United States Navy
B.S., United States Naval Academy, 1967

Submitted in partial fulfillment of the
requirements for the degree of

MASTER OF SCIENCE IN AERONAUTICAL ENGINEERING

from the

NAVAL POSTGRADUATE SCHOOL
March 1973

ABSTRACT

The present concept of automatic throttle control, as employed in
Navy carrier-based aircraft, was investigated. The aircraft chosen for
study was the A-7E. The powerplant was the TF41-A-2, a turbofan engine
with a relatively slow throttle response in the approach power range.

The effects of additional inputs to the approach power compensator
were evaluated. It was shown that a considerable increase in performance
could be achieved through the incorporation of longitudinal feedback.
In addition, the limitations imposed on performance by large engine lags
were found to be much less severe for systems with longitudinal feedback.
The modifications suggested require a redesign of the approach power
compensator system currently in use by the Navy.

TABLE OF CONTENTS

TABLE OF CONTENTS (continued)

LIST OF TABLES

ACKNOWLEDGEMENT

I. INTRODUCTION

A. APCS PERFORMANCE OBJECTIVES

The primary purpose of an approach power compensator system (APCS) in Navy carrier-based aircraft is to provide the thrust necessary to maintain the correct airspeed during carrier approach and landing. The APCS can be used either in an automatic carrier landing system (ACLS) or in a piloted, manual approach. Although airspeed systems exist [Ref. 1], the systems utilized in Navy aircraft attempt to maintain a constant angle of attack (AOA). Supplementary inputs, such as normal acceleration and elevator crossfeed, are usually employed in an effort to maintain the "on-speed" AOA. Since the on-speed value of AOA does not vary from approach to approach, there is no indexing requirement. In an airspeed system, however, the reference airspeed is a function of the aircraft configuration in the landing approach. As configuration variables, such as weight, vary from approach to approach, so does the reference airspeed. This is an important factor in favor of an AOA system. The pilot workload which airspeed indexing would add to an already demanding task probably would not be tolerated, and the designer of an approach power compensator system should bear this in mind.

Military specifications reflect the objective of maintaining a constant AOA. Reference 2 states that the output of the APCS shall be proportional to error in AOA, change in normal acceleration, integral of AOA error, and elevator position. As is noted in Ref. 1, it appears that the APCS design concept is overly restricted by military specifications. However, these specifications do point out the current Navy APCS concept.

B. AIRCRAFT

The aircraft chosen for study was the A-7E, a light-attack, carrier-based aircraft of approximately 20,000 pounds empty gross weight. The A-7E was chosen because it was one of two aircraft included in a previous study of Navy approach power compensator problems and requirements [Ref. 1] and because the author has had personal experience as an A-7A pilot.

The A-7E powerplant is a turbofan engine whose throttle response is characterized by a relatively long and nonlinear time constant in the approach thrust range. The APCS is an AOA system with inputs of AOA, integral of AOA, normal acceleration, and unit horizontal tail (UHT) movement. A detailed description of the system is contained in Ref. 3.

C. PREVIOUS STUDIES

Systems Technology, Incorporated conducted a study of Navy approach power compensator problems and requirements [Ref. 1]. The following is a summary of pertinent conclusions and recommendations:

1. A fundamental conceptual difficulty with current APCS's is the use of AOA feedback to constrain both AOA and airspeed, as the two are only in phase at low frequencies. Thus, it is possible to control only one of these or a linear combination of the two with a single control input. As a consequence, APCS design involves a compromise between these constraints.

2. Airframe characteristics restrict the ability to achieve satisfactory performance. Engine response time is a fundamental problem area, as the APCS cannot augment the dynamics without excessively overdriving the engine. It was recommended that the effect of engine lag on APCS performance be investigated in detail with a view toward specifying necessary characteristics.

3. Gust response within the current APCS concept will, in general, be poor. Gust proofing against longitudinal gusts with an AOA system is difficult. Gust proofing against vertical gusts has minimal effect, as the dominant response is determined by the short period characteristics.

4. It was recommended that the effects of additional feedbacks to the APCS be analyzed in relation to gust response and to optimum performance for separate configurations of fully automatic and manually controlled systems.

The Naval Air Test Center conducted an evaluation of the APCS in

the A-7E [Ref. 3]. The emphasis was on optimizing the performance of

the APCS for both manual and ACLS approaches with minimal material and

design modifications. The recommended modifications were basically

changes in feedback gains and the incorporation of a dual time constant

in the UHT crossfeed circuit. A shorter time constant was used for

nose up corrections than for nose down corrections, with the net result

that the UHT input was more effective for nose up than for nose down

attitude changes.

D. OBJECTIVES

The purpose of this research was to improve the performance of the

APCS of the A-7E aircraft as used in the ACLS. Specifically, the

effects of additional inputs to the APCS computer were evaluated with a

goal of improving the current concept of APCS design. In addition, the

effect of engine response time on APCS performance was determined.

II. METHOD OF ANALYSIS

A. DESCRIPTION OF THE MODEL

The fully automatic carrier landing mode was selected for study in this analysis of the APCS. The manual mode with the pilot in the loop was not considered. Thus, the total closed loop system consisted of the airframe, the engine, the approach power compensator, the longitudinal automatic flight control system (AFCS), and the automatic carrier landing system.

The aircraft equations of motion were linearized about the steady state approach conditions in accordance with standard small perturbation theory, as described by Etkin [Ref. 4]. Lateral-directional dynamics were not included. The resultant equations are shown in Figure 1. Aircraft stability derivatives and other parameter values were taken from Ref. 1 and are listed in Table I. Force and moment stability derivatives are normalized with respect to mass and moment of inertia, respectively. Hence, mass and moment of inertia do not appear explicitly in the equations of motion, as they do in Etkin's notation.

The A-7E engine is the TF41-A-2 turbofan. Reference 5 contains an analysis of the thrust-power lever relationship for a range of operating conditions. The nominal approach thrust for the operating conditions as shown in Table I is 3000 pounds. In this range of thrust, the engine response time constant is a nonlinear function of thrust. The relationship between the engine time constant, T_e, and thrust, and the relationship between thrust and power lever angle (δ_{PLA}) for the given operating conditions are taken from Ref. 1 and are shown in Figure 2. An average value of 275 pounds thrust per degree δ_{PLA} was used in the model. Thus, the variable engine lag was the only nonlinearity in the engine model.

11

Figure 3 is a schematic of the APCS loop closures. In small perturbation theory, AOA is defined as w/U_0, in radians. Thus, the inputs to the APCS computer are proportional plus integral w, a'_z (vertical acceleration corrected for accelerometer location), and a filtered UHT feedforward term.

The APCS gains are a representative set listed as "PAX" gains in Ref. 1 and do not correspond exactly to those in use in the current A-7E APCS configuration. In addition, several simplifications were made to the APCS model. A complex pole at ten rad/sec in the throttle actuator response was neglected. This frequency is well beyond the range in which the APCS is effective. Throttle linkage hysteresis of 0.5 degrees was ignored. The implementation of a dual UHT input time constant, as described in the introduction, was not incorporated into the model. A gain adjust bias exists in the APCS which changes all APCS gains by the same amount to compensate for ambient air temperature effects. The standard day value of 1.0 was used. K_{n_z}, the vertical acceleration gain, has two values, the smaller value being for load factors in excess of 1.1 g's. Only the larger value was incorporated into the model.

Both the longitudinal AFCS and the ACLS models were taken from Ref. 6. As above, the AFCS and ACLS gains were representative but were not necessarily identical to those currently in use. A complex pole and a first order lag at 20 rad/sec in the AFCS response was neglected. The AFCS output is a UHT deflection, which is a function of attitude error $(\theta - \theta_c)$, pitch rate, and normal acceleration. The automatic carrier landing system was represented by the A-7E SPN-42 longitudinal control equation. The output, a ship-to-aircraft pitch command, is a function of the aircraft altitude error, Z_e, measured perpendicular to the ideal

glide slope. In practice, the aircraft slant range and elevation are measured by the SPN-42 radar, corrected for ship motion and radar location, transformed into cartesian coordinates, and utilized to command an aircraft pitch angle.

The AFCS and ACLS longitudinal control equations are shown in Figure 4. APCS, AFCS, and ACLS gains are listed in Table II.

B. DIGITAL SIMULATION

1. Continuous System Modeling Program

The closed loop system was simulated on the IBM 360 digital computer utilizing a digital simulation language, CSMP. CSMP is an acronym for Continuous System Modeling Program. The program is augmented by basic FORTRAN and provides a set of functional blocks which simulate such analog components as integrators, relays, and function generators. A detailed description of the program is contained in Ref. 7. A description of CSMP functions used in the simulation is provided in Table III.

2. CSMP Program Components

A sample program and output are contained in Appendix A. The program consists of five major sections: the aircraft equations of motion and engine model, the APCS model, the AFCS model, the ACLS model, and a gust input model.

a. Aircraft Equations of Motion and Engine Model

The equations of motion as shown in Figure 1 were put into state format:

$$\{\dot{X}\} = [A] \{X\} + [B] \{R\}$$
$$\{Y\} = [C] \{X\} + [D] \{R\} + [E] \{Y\}$$

(1)

where:

$$\{X\} = \begin{Bmatrix} u \\ w \\ \theta \\ q \end{Bmatrix} \qquad \{Y\} = \begin{Bmatrix} \dot{h} \\ a_z \\ a'_z \end{Bmatrix} \qquad \{R\} = \begin{Bmatrix} \delta_e \\ \Delta T \\ u_g \\ w_g \end{Bmatrix} \quad (2)$$

The A, B, C, D, and E matrices are listed in Table IV.

The engine modeling consisted of two parts. As mentioned in section II.A., a relationship of 275 pounds thrust per degree δ_{PLA} was assumed. The engine time constant, as shown in Figure 2, was approximated by a linear function generator of fifteen unequally spaced points. The thrust operating range modeled was ±2000 pounds about the nominal operating value of 3000 pounds.

b. APCS Model

The APCS equations were obtained from Figure 3. The throttle actuator, power lever, and engine gains were combined into a single parameter. As a result, the variable labeled "PLA" in the CSMP program is not the actual power lever angle. Gains and other constants in the feedback loops were also consolidated wherever possible. AOA and integral of AOA were kept distinct. For ease of programming, the δ'_e/δ_e transfer function was written as

$$\frac{\delta'_e}{\delta_e}(s) = \frac{K_{\delta_e} T_w s}{T_w s + 1} = \frac{1}{s + 1/T_w} \cdot K_{\delta_e} s \equiv \frac{W1}{\delta_e} \cdot \frac{\delta'_e}{W1} \quad (3)$$

The UHT input equations in the simulation are in the form of the right side of Equation (3).

c. AFCS Model

The AFCS equations were obtained from the equation given in Figure 4 with numerical values substituted for the various gains.

d. ACLS Model

The altitude error, Z_e, was defined as the negative of h, as the two are measured in opposite directions perpendicular to the ideal glideslope. The θ_c/Z_e transfer function, as shown in Figure 4, was rearranged for programming as follows:

$$\frac{\theta_c}{Z_e}(s) = \frac{K_c K_x}{K_p s + 1}\left\{\left[\frac{\frac{s}{3.9}+1}{\left(\frac{s}{5}\right)^2+\frac{s}{3.5}+1}\right]\left[\frac{t_i K_x}{s}+1\right]+\left[\frac{R_x s}{\left(\frac{s}{5}\right)^2+\frac{s}{3.5}+1}\right]t_r\right\} \quad (4)$$

$$= K \cdot \frac{s^2+a_1 s+a_0}{s(s+1/K_p)(s^2+7.14s+25.0)}$$

where

$$K = \frac{K_c K_x(97.5R_x t_r+25.0)}{3.9K_p}$$

$$a_1 = \frac{3.9+t_i K_x}{3.9R_x t_r+1.0} \qquad\qquad a_0 = \frac{3.9t_i K_x}{3.9R_x t_r+1.0}$$

Finally

$$\frac{\theta_c}{Z_e}(s) = \frac{K}{s}\cdot\frac{s^2+a_1 s+a_0}{s^3+b_2 s^2+b_1 s+b_0} \equiv \frac{Z_i}{Z_e}\cdot\frac{\theta_c}{Z_i} \quad (5)$$

where

$$b_2 = \frac{1}{K_p}+7.14 \qquad b_1 = \frac{7.14}{K_p}+25.0 \qquad b_0 = \frac{25.0}{K_p}$$

15

The SPN-42 equations in the simulation are in the form of the right side of Equation (5).

e. Gust Model

To simulate a random gust field, the output of a random number generator with a uniform amplitude distribution was passed through a second-order filter with a break frequency of 1.0 rad/sec and a damping ratio of 0.707. The theoretical derivation of the spectral properties of the resultant signal is described in Appendix B. Vertical and horizontal RMS gust velocities of 5.0 ft/sec were used in the simulation. To insure identical gust signals for each run, a constant step size was used in the numerical integrations for all runs.

f. RMS Velocity Error Criteria

An RMS velocity error for u and w was used as a measure of APCS effectiveness. It was defined as:

$$E_{RMS} = \left[\frac{1}{T} \int_0^T [u(t)^2 + \dot{w}(t)^2] dt \right]^{\frac{1}{2}} \tag{6}$$

where T is the run length.

g. Digital Simulation Error Analysis

A fourth-order Runge-Kutta numerical integration scheme with a fixed step size was used in the simulation. Figure 5 is a plot of normal acceleration after 0.5 seconds versus step size for an initial altitude error. Plots of other system variables, after 0.5 seconds and at other values of time, show the same trend. A step size of 0.05 seconds was chosen for the simulation.

C. THEORETICAL ANALYSIS

The theoretical analysis was primarily a root locus study of various APCS configurations. To reduce the multiple input, multiple output control system to a form adaptable to the analysis, a multiple loop analysis technique, documented in Ref. 8, was employed. An explanation of the method, including an example which covers all applications used in this study, is contained in Appendix C. Table V is a listing of the open loop aircraft numerators, cross product numerators, and the open loop denominator used in the analysis.

III. PROCEDURE

A. DIGITAL SIMULATION RUNS

.A standard set of runs for the digital simulation was utilized for each configuration of the APCS. The APCS configuration shown in Figure 3 is referred to as the standard configuration. The length of the simulation runs was chosen to approximate the final approach phase of the carrier landing. Under SPN-42 control, two of the ACLS equation gains, R_x and K_x, are functions of range for a range greater than 6000 ft. For ranges less than 6000 ft. the values of R_x and K_x are constant at the values shown in Table II. The ACLS equation employed was valid for range less than 6000 ft. to the point at which deck motion compensation is introduced. A run time of 30 seconds was chosen to approximate this phase of the approach. A set of six standard simulation runs was chosen to simulate system response to initial high and low airspeed and altitude errors and to vertical and longitudinal gust inputs. The set of conditions for the six runs were:

Run   (1) $u(0)$ =   5 ft/sec, $w(0)$ = -5 ft/sec

       (2) $u(0)$ = - 5 ft/sec, $w(0)$ =   5 ft/sec

       (3) $Z_e(0)$ =   10 ft

       (4) $Z_e(0)$ = -10 ft

       (5) $\bar{u}_g$ =   5 ft/sec

       (6) $\bar{w}_g$ =   5 ft/sec

Initial conditions and RMS gust velocities not specifically indicated in a run are zero.

B. ANALYSIS OF THE STANDARD APCS CONFIGURATION

To apply the analysis technique described in Section II.C, the APCS loop closures as shown in Figure 3 were reduced to an equivalent set that conformed to the block diagram format shown in Figure C.1. The equivalent transfer functions were a consolidation of all the elements in each loop closure, including the thrust to power lever terms. The resultant diagram is shown in Figure 6. G_w represents the proportional plus integral AOA feedback transfer function and is given by

$$G_w = - \frac{57.3 \cdot 1.389}{U_0} \left(\frac{K_\alpha}{T_\alpha s + 1} + \frac{K_{\alpha_I}}{s} \right) \cdot \frac{350.7}{T_e(s + 1/T_e)}$$

$$= \frac{-350.7 \cdot 57.3 \cdot 1.389 \left(\frac{K_\alpha}{T_\alpha} + K_{\alpha_I} \right) \left(s + \frac{K_{\alpha_I}}{K_\alpha + K_{\alpha_I} T_\alpha} \right)}{U_0 T_e s (s + 1/T_\alpha)(s + 1/T_e)} \tag{7}$$

Numerically

$$G_w = - \frac{1021.5(s + 0.197)}{T_e s (s + 2.857)(s + 1/T_e)}$$

G_z represents the normal acceleration feedback transfer function. The effect of the 6.7 ft. offset of the accelerometer on APCS performance has been shown to be minor in the low frequency range [Ref. 1]. Thus, the offset was neglected in the equivalent system, simplifying the analysis.

$$G_z = - \frac{K_{n_z} \cdot 350.7}{32.2 \cdot T_e (s + 1/T_a)(s + 1/T_e)}$$

$$\tag{8}$$

$$= - \frac{327.2}{T_e(s + 1)(s + 1/T_e)}$$

19

G_{δ_e} represents the UHT crossfeed transfer function and is given by

$$G_{\delta_e} = -\frac{K_{\delta_e} \cdot 350.7s}{T_e(s+1/T_w)(s+1/T_e)}$$

$$= -\frac{50,235s}{T_e(s+0.435)(s+1/T_e)}$$

$$(9)$$

The theoretical analysis was confined to the APCS loop closures only; AFCS and ACLS loop closures were not considered. Justification for this procedure is given in Section IV.B.

The closed loop transfer functions u/δ_e, w/δ_e, and u/u_g for the standard APCS configuration were formed. The engine time constant, T_e, was kept as a parameter, and root locus plots of the zeroes of the closed loop denominator and numerators were plotted to show the effects of engine lag.

Since there are two feedback paths, as shown in Figure 6, the closed loop denominator is defined as Δ''. It was derived by applying equation C.5.

$$\Delta'' = \Delta + G_w N_{\Delta T}^w + G_z N_{\Delta T}^{a_z} \tag{10}$$

$N_{\Delta T}^{a_z}$ was expanded as

$$N_{\Delta T}^{a_z} = N_{\Delta T}^{(sw-U_0 s\theta)} = s N_{\Delta T}^w - U_0 s N_{\Delta T}^\theta \tag{11}$$

Equation 11 was substituted into Equation 10 to yield

$$\Delta'' = \Delta + G_w N_{\Delta T}^w + s G_z (N_{\Delta T}^w - U_0 N_{\Delta T}^\theta) \tag{12}$$

The expression was cleared over a common denominator, and the numerator expressed in two terms, one a function of T_e, to give

$$\Delta'' = \frac{U + 1/T_e V}{s(s+1)(s+2.857)(s+1/T_e)} \tag{13}$$

where

$$U = s^2(s+1)(s+2.857)\Delta$$

$$V = s^7+4.913s^6+9.241s^5+10.91s^4+6.153s^3+1.240s^2$$
$$+0.1810s-0.007699$$

The zeroes of Δ'' were plotted as a function of $1/T_e$ by forming an artificial transfer function, G, given by

$$G \equiv \frac{1/T_e V}{U} \tag{14}$$

G represents the open loop transfer function in a unity feedback, single loop system. This form was adaptable to a documented root locus digital computer program [Ref. 9]. The closed loop characteristic equation for the artificial system was

$$\Delta' = U + 1/T_e V \tag{15}$$

$1/T_e$ equal to zero represents an infinite engine lag, hence, a no thrust condition. Thus, the root loci originate at the open loop phugoid, short period, and control equation roots. The zeroes of the artificial closure represent the roots that would be obtained for the given APCS feedback gains if there were no engine delay. Figure 7 is a plot of the root loci. Only the loci above and on the real axis are shown. An

engine delay of 1.8 seconds occurs at the nominal operating thrust of 3000 pounds. This value and the values at thrust levels of ±2000 pounds about the nominal value are indicated on Figure 7.

Closed loop numerator zeroes were plotted for $N_{\delta_e}^u\Big]_{std}$, $N_{\delta_e}^w\Big]_{std}$, and $N_{u_g}^u\Big]_{std}$, where the subscript "std" refers to the loop closures for the standard configuration.

$$N_{\delta_e}^u\Big]_{std} = N_{\delta_e}^u + G_z N_{\delta_e\Delta T}^{u \ a_z} + G_w N_{\delta_e\Delta T}^{u \ w} + G_{\delta_e} N_{\Delta T}^u$$

$$= \frac{U + 1/T_e V}{s(s+1)(s+2.857)(s+0.435)(s+1/T_e)} \tag{16}$$

where

$$U = s^2(s+1)(s+2.857)(s+0.435)N_{\delta_e}^u$$

$$V = -65.43s^7 - 318.6s^6 - 542.8s^5 - 1024.6s^4 - 718.8s^3$$

$$-87.79s^2 + 0.2346 + 1.707$$

Figure 8 is a plot of the zeroes of $N_{\delta_e}^u\Big]_{std}$ for $1/T_e$ variation.

$$N_{\delta_e}^w\Big]_{std} = N_{\delta_e}^w + G_w N_{\delta_e\Delta T}^{w \ \ \ 0} + sG_z N_{\delta_e\Delta T}^{w \ \ 0} - sG_z U_0 N_{\delta_e\Delta T}^{w \ \theta} + G_{\delta_e} N_{\Delta T}^w$$

$$= \frac{U + 1/T_e V}{s(s+1)(s+0.435)(s+1/T_e)} \tag{17}$$

22

$$U = s(s+1)(s+0.435)N^w_{\delta_e}$$

$$V = -2.155s^5 - 511.6s^4 - 782.7s^3 - 343.6s^2 - 68.90s - 8.753$$

Figure 9 is a plot of the zeroes of $N^w_{\delta_e}\Big]_{std}$ for $1/T_e$ variation.

$$N^u_{u_g}\Big]_{std} = N^u_{u_g} + G_w N^{u\ w}_{u_g \Delta T} + G_z N^{u\ a_z}_{u_g \Delta T}$$

$$= \frac{U + 1/T_e V}{s(s+2.857)(s+1)(s+1/T_e)} \tag{18}$$

$$U = s^2(s+2.857)(s+1)N^u_{u_g}$$

$$V = 0.05453s^6 + 0.2789s^5 + 1.058s^4 + 1.716s^3 + 1.141s^2 + 1.797s - 0.007686$$

Figure 10 is a plot of the zeroes of $N^u_{u_g}\Big]_{std}$ for $1/T_e$ variation.

C. INVESTIGATION OF ADDITIONAL APCS INPUTS

In studying the effects of additional APCS feedback variables, T_e was fixed at the nominal value of 1.8 seconds. The closed loop denominator and numerators evaluated at this value are shown in Table VI. The additional feedback variables which were considered were combinations of proportional, integral and derivative of longitudinal velocity, u. As a result, the closed loop u/u_g and u/δ_e transfer function zeroes were not affected. Subsequent to each root locus analysis, a set of digital simulation runs, as described in Section III.A, were completed with the altered configuration. A summary of the RMS velocity errors is contained in Table VII.

Longitudinal acceleration feedback was first considered. The equivalent transfer function for $\dot{u}$ feedback, defined as $G_{\dot{u}}$, is

$$G_{\dot{u}} \equiv \frac{350.7 K_{\dot{u}}}{T_e(s+1/T_e)}$$

With T_e equal to 1.8 seconds, this becomes

$$G_{\dot{u}} = \frac{194.8 K_{\dot{u}}}{s+0.56} \tag{19}$$

The closed loop denominator, defined as Δ''', was formed by modifying Δ'' as follows:

$$\Delta''' = \Delta'' + G_{\dot{u}} N_{\Delta T}^{su} \tag{20}$$

Figure 11 is a root locus plot of the zeroes of Δ''' as $K_{\dot{u}}$ was varied.

In a like manner, longitudinal velocity feedback was considered.

$$G_u \equiv \frac{194.8 K_u}{s+0.56} \tag{21}$$

The closed loop denominator was again defined as Δ'''.

$$\Delta''' = \Delta'' + G_u N_{\Delta T}^{u} \tag{22}$$

Figure 12 is a plot of the zeroes of Δ''' as K_u was varied.

A combination of proportional plus integral longitudinal velocity was considered next.

$$G_{\hat{u}} \equiv \frac{194.8}{s+0.56} \cdot K_u(1+K_p/s) \tag{23}$$

Values of K_p from 0.1 to 0.5 were considered. Figure 13 is a plot of the zeroes of Δ''' as K_u was varied with K_p equal to 0.5.

The final configuration considered was proportional plus derivative of longitudinal velocity.

$$G_{\bar{u}} = \frac{194.8}{s+0.56} \cdot K_{\dot{u}}(s+K_q) \tag{24}$$

Figure 14 is a plot of the zeroes of Δ''' as $K_{\dot{u}}$ was varied with values of K_q equal to 0.2, 0.5, and 1.0. The phugoid roots are indicated for all three values of K_q. The closed loop numerator for the w/δ_e transfer function was formed.

$$N_{\delta_e}^w \Big]_{rev} = N_{\delta_e}^w + G_{\bar{u}} N_{\delta_e}^w{}_{\Delta T}^u \tag{25}$$

The subscript "rev" refers to revised configuration. The resultant root loci for K_q equal to 0.5 are shown in Figure 15.

D. REVISED APCS CONFIGURATION

Based on the results of the investigation of various inputs, a final APCS configuration was chosen. As compared to the standard system, this configuration had additional inputs of proportional plus derivative of longitudinal velocity with specific gains of 0.5 and 2.0 for K_q and $K_{\dot{u}}$, respectively. The revised equivalent APCS block diagram is shown in Figure 16.

With the gains fixed at the values given above, root locus plots for the zeroes of Δ''' and $N_{\delta_e}^w \Big]_{rev}$ for $1/T_e$ variation were plotted and are shown in Figures 17 and 18, respectively.

Straight-line approximations to Bode plots for u/δ_e, w/δ_e, and u/u_g were constructed for comparing the standard and revised APCS

configurations. The transfer functions are listed in Table VIII, and
the magnitude portion of the Bode plots are shown in Figures 19 through
21.

IV. DISCUSSION AND RESULTS

A. EFFECTS OF ENGINE RESPONSE

Strictly speaking, the incremental root locus technique showing how the poles and zeroes of the APCS-equipped aircraft vary with the non-linear engine time constant is not valid. The use of root locus analyses is valid only for linear systems. However, an incremental root locus technique has been used for stability analyses of systems with single-valued continuous nonlinearities [Ref. 10]. The system response is approximately defined by the instantaneous location of the roots, here a function of the instantaneous thrust.

The initial conditions and the gust inputs used in the simulation were considered to be representative of those that an APCS/aircraft system would be expected to encounter. Visual inspection of system response curves did not reveal the thrust response nonlinearity; i.e., the curves were approximately sinusoidal in shape, indicating that the system performance could be evaluated by considering a fixed value of T_e equal to 1.8 seconds. The minor effect of the nonlinearity was due to the low variance of ΔT in relation to the size of the thrust operating range modeled. The dependence of the response on T_e was greater for the revised system, as can be seen by comparing Figures 7 and 9 with Figures 17 and 18. This was a direct result of the increased capability to alter APCS performance with the longitudinal feedback.

The analysis did not provide insight concerning the specific effects of a large engine lag on APCS performance. However, the limitations imposed on performance by a large engine lag were shown to

be less severe for a system incorporating longitudinal feedback. As reported in Ref. 1, the larger feedback gains or lead compensation necessary to improve the standard AOA system performance result in excessively overdriving the engine. The longitudinal feedback provided an increase in performance and a more efficient use of the engine. The thrust response induced was directly related to the damped natural frequency of the phugoid mode. As the frequency was increased, as in Figure 12 for increasing K_u , peak to peak thrust values increased as well. However, for configurations in which the damped natural frequency was not appreciably increased, as in Figures 11 and 14, peak to peak thrust values were less than those for the standard configuration.

B. EFFECTS OF ADDITIONAL APCS INPUTS

As mentioned in Section III.B, the theoretical analysis neglected AFCS/ACLS loop closures. It was shown that these closures do not appreciably effect airspeed response for the system under study. Phugoid damping coefficients and damped natural frequencies were taken from the root locus plots of Figures 11 through 14. Measurements of the period and the time to one half initial amplitude of the airspeed responses were then made for the closed loop simulations, which included AFCS and ACLS closures. The damped frequencies and damping coefficients calculated from these responses were within a few per cent of those predicted by the root locus plots. Thus, it was concluded that airspeed response as controlled by the APCS was not significantly altered by AFCS and ACLS loop closures.

1. Longitudinal Acceleration

Only a limited increase in performance was achieved by the implementation of u feedback, as only a minimal increase in phugoid damping could be achieved.

28

2. Longitudinal Velocity

The addition of u feedback increased the absolute phugoid damping but provided only a minor increase in the damping coefficient and, therefore, no decrease in per cent overshoot. The most important factor was the increased damped natural frequency. It was considered necessary to keep the damped frequency near the level of that of the standard configuration, as a much higher value would prove unacceptable due to the rapid oscillations in thrust which would result.

3. Proportional Plus Integral Longitudinal Velocity

The inclusion of an integral term had an adverse effect on airspeed response for an initial airspeed error. This was predicted by the root locus plot as shown in Figure 13. The response to a longitudinal gust field was observed to be improved, as documented in Table VII. This shows up in the root locus plots of Figures 10 and 13 as an approximate cancellation of the phugoid poles with u/u_g zeroes.

4. Longitudinal Velocity Plus Acceleration

The inclusion of a combination of proportional plus derivative of longitudinal velocity in the APCS provided the best increase in over-all system performance. For values of K_q greater than 0.5, the damped frequency increases substantially with the feedback gain, $K_{\dot{u}}$. For a value of K_q equal to 0.5 a large increase in damping was achieved while the damped frequency was held nearly constant. Improvement of APCS performance rapidly diminished as K_q was reduced below 0.5.

A stable first-order pole was shown to approach the origin as longitudinal feedback gains were increased [Figures 12 and 14], and its presence was evident in the digital simulations. For the configuration described in Section IV.B4 with an initial airspeed error, a residual

airspeed error of opposite sign and with a value of ten per cent of the

initial airspeed error remained and slowly decayed after the phugoid

had essentially damped out. The effect of the pole was considered to

be of minor significance. As shown in Figure 15, there was a correspond-

ing zero in the w/δ_e numerator. Consequently, the first order pole did

not appear in the angle of attack response.

C. FINAL CONFIGURATION

The choice of the final, revised configuration was based on several

factors: phugoid damping, damped natural frequency and gust response.

A combination of longitudinal velocity and acceleration inputs was the

only combination able to provide a substantial increase in phugoid

damping while maintaining a constant damped natural frequency. The

choice of the value of $K_{\dot{u}}$ was somewhat arbitrary. For a value of 2.0

the effective longitudinal velocity feedback gain was 1.0, which was of

the same magnitude as K_{α} in units of volts per ft/sec; at a higher

value of $K_{\dot{u}}$ the airspeed input becomes dominant over AOA. Improved

performance at a larger value of $K_{\dot{u}}$ was indicated by the root locus

plot and was verified by simulation [Table VII].

Longitudinal gust response was substantially improved for all

configurations with longitudinal feedback. The most significant improve-

ments, as indicated by the RMS velocity errors, were achieved for the

configurations in which the damped natural frequency was increased over

that of the standard configuration. The ratio of u to $\dot{u}$ feedback chosen

represented a tradeoff between gust response and frequency criteria.

Vertical gust response as measured in simulation was not appreciably

altered. As that was expected prior to the study (Section I.C), there

was no theoretical analysis attempted in that area.

30

For an initial altitude error for all configurations, the induced airspeed error was primarily an AOA, or $w(t)$, transient which decays in five seconds. The induced airspeed error, $u(t)$, was much smaller in comparison. Thus, the addition of the longitudinal feedbacks have a negligible effect on responses induced by an initial altitude error. Based on this result, it was concluded that airspeed response at push-over from level flight to glideslope acquisition would be unaltered.

The frequency response plots of Figures 19 through 21 indicate the frequency range which was modified by the APCS revision. The amplitude plots for u/δ_e and u/u_g indicate this range was from 0.07 to 0.5 rad/sec, while only the amplitudes at low frequencies were attenuated in the w/δ_e plot. The additional favorable effect of an approximate three dB attenuation at the phugoid break frequency of the revised configuration was not indicated on the asymptotic plots.

V. CONCLUSIONS AND RECOMMENDATIONS

A. APCS CONFIGURATION

Substantial improvement in performance is possible through the use
of longitudinal feedback. However, only an acceleration term can be
practically obtained with the current APCS, as it would entail only the
implementation of an accelerometer signal. Once an airspeed feedback
is considered, the need for an airspeed reference is required, necessitat-
ing a major APCS redesign. An airspeed reference, manually set by the
pilot, would not be acceptable. In addition to the added pilot respon-
sibility mentioned in Section I, the combined AOA/airspeed system
references would require airspeed reference accuracy greater than the
pilot could be expected to provide.

In summary, only limited improvement in performance is possible
within current limitations. It is recommended that the current APCS
design concept be considered for revision. Present day aircraft, such
as the A-7E and the F-14A/B, have precise airspeed measuring equipment
(air data computers) and digital computers on board. The possibility
of utilizing those devices to accurately measure and reference airspeed
for its incorporation into the APCS should be studied.

The possible improvement of gust response gained by the revised
APCS configuration is partially governed by the method of sensing air-
speed. If an inertial device is utilized, the actual airspeed, u, is
measured, but the term $(u-u_g)$ is measured if an air data computer is
utilized. The effect of including the gust velocity in the sensed
airspeed signal was to degrade performance below that gained by the
revised configuration (e.g., the RMS value of velocity error for a

32

horizontal gust input was 4.1 ft/sec.   With the gust velocity included

in the feedback signal, the error was 5.0 ft/sec, still substantially

improved over the original value of 6.3 ft/sec).

Angle of attack response was not degraded by the inclusion of

longitudinal feedback but, in fact, was improved.

B.   ENGINE RESPONSE

The effect of the nonlinear engine time constant on APCS performance

was shown,to be minor for the range of operating conditions considered.

The limitations imposed on APCS performance by a large engine lag

are much less severe for a system incorporating longitudinal velocity

and acceleration feedback than for the standard angle of attack config-

uration.

C.   THEORETICAL ANALYSIS

Restricting the multiple loop control system analysis technique to

the APCS loop closures was shown to be valid for an evaluation of air-

speed control. The implementation of the method provided a systematic

approach for the study of APCS performance.

D.   GENERALIZATION OF RESULTS

The choice of a single APCS/aircraft system for the analysis may

restrict the validity of some of the results to that particular system.

However, as all current Navy APCS's use the same basic AOA system, it

is postulated that the general concept presented is applicable to other

aircraft. Correlation of results with other systems should be attempted.

The study was restricted to the fully automated carrier landing

mode. The validity of the results for a pilot-controlled attitude loop

should be investigated.

REFERENCES

[1]   Systems Technology, Inc. Report 197-1, <u>An Analysis of Navy Approach</u>
      <u>Power Compensator Problems and Requirements</u>, by S. J. Craig,
      R. F. Ringland, and I. L. Ashkenas, March 1971.

[2]   Department of the Navy Military Specification MIL-23866A(WP),
      <u>Control Set, Approach Power AN/ASN-54 (V)</u>, 15 September 1965.

[3]   Naval Air Test Center Report FT-16R-71, <u>Evaluation of the Approach</u>
      <u>Power Compensator System in the A-7E Airplane</u>, by Lcdr W. C. Bowes,
      USN, A. P. Schust, Jr., and J. L. Griffith, 19 March 1971.

[4]   Etkin, B., <u>Dynamics of Flight</u>, Wiley, 1959.

[5]   Naval Air Propulsion Test Center Report ATD-211, <u>TF41-A-2 Engine</u>
      <u>Thrust-Power Lever Relationship</u>, by P. F. Piscopo, January 1972.

[6]   Naval Air Test Center Report FT-28R-72, <u>Development of the A-7E</u>
      <u>Airplane Automatic Carrier Landing System (ACLS) Mode I Operational</u>
      <u>Capability</u>, by Lt W. B. Christie, USN and A. P. Schust, Jr., 11 May
      1972.

[7]   IBM Application Program 360A-CX-16X, <u>System/360 Continuous System</u>
      <u>Modeling Program User's Manual</u>, 4th ed., IBM Corporation, October
      1969.

[8]   Air Force Flight Dynamics Laboratory Report TDR-62-1014, <u>Analysis</u>
      <u>of Multiloop Vehicular Control Systems</u>, by D. T. McRuer, I. L.
      Ashkenas, and H. R. Pass, March 1964.

[9]   Air Force Flight Dynamics Laboratory Report FDCC TM 69-4, <u>User's</u>
      <u>Manual for a Digital Computer Routine to Calculate Root Loci</u>, by
      F. L. George and Capt J. D. Fisher, USAF, December 1969, Revised
      October 1971.

[10] Thaler, G. H., DR. ENG. and Pastel, M. P., Ph.D. <u>Analysis and</u>
      <u>Design of Nonlinear Feedback Control Systems</u>, McGraw Hill, 1962.

TABLE   I

AIRCRAFT GEOMETRY AND STABILITY DERIVATIVES

STABILITY DERIVATIVES		APPROACH PARAMETERS	
X_u	- 0.05435	S	375 ft^2
X_w	0.064327	W	24,000 lb
Z_u	- 0.286953	I_{yy}	68,000 slug-ft^2
$Z_{\dot{w}}$	0	MAC	10.84 ft
Z_w	- 0.528871	m	746 slugs
M_u	- 0.000165	h	Sea Level
$M_{\dot{w}}$	- 0.000289	ρ	0.002378 $\frac{slugs}{ft^3}$
M_w	- 0.007964	U_0	218 ft/sec
M_q	- 0.327532	α_0	12 deg
X_{δ_e}	0.732836	c.g.	28.6 % MAC
Z_{δ_e}	-14.713536	l_x	6.7 ft (ahead of c.g.)
M_{δ_e}	- 2.188878		
$X_{\Delta T}$	0.001317		
$Z_{\Delta T}$	- 0.000250		
$M_{\Delta T}$	0.000004		

TABLE II

CONTROL SYSTEMS PARAMETERS

AFCS		APCS	
K_θ	1.9 rad/rad	K_{δ_e}	143.2 volts/rad
$K_{\dot\theta}$	1.0 rad/rad-sec	T_w	2.3 sec
K_{n_z}	3.0 deg/g	$K_{\alpha'}$	2.6 volts/unit α
		K_{α_I}	0.55 volts/unit-sec
		T_α	0.35 sec

ACLS			
K_c	1/5.4	K_{n_z}	30.0 volts/g
K_x	1.0	T_a	1.0 sec
K_p	0.376		
R_x	1.0		
t_i	1/15		
t_r	2.5		

TABLE III

CSMP FUNCTIONAL BLOCKS
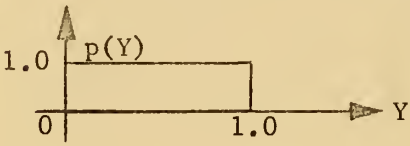
General Form	Function
$Y = INTGRL(IC,X)$ $Y(0) = IC$ Integrator	$Y = \int_0^t Xdt + IC$ Laplace Transform: $\dfrac{1}{s}$
$Y = REALPL(IC,P,X)$ $Y(0) = IC$ 1st Order Lag	$P\dot{Y} + Y = X$ Laplace Transform: $\dfrac{1}{Ps + 1}$
$Y = CMPXPL(IC_1,IC_2,P_1,P_2,X)$ $Y(0) = IC_1$ $\dot{Y}(0) = IC_2$ Complex Pole	$\ddot{Y} + 2P_1P_2\dot{Y} + P_2^2 Y = X$ Laplace Transform: $\dfrac{1}{s^2 + 2P_1P_2s + P_2^2}$
$Y = AFGEN(FUNCT,X)$ Arbitrary Function Gener- ator(Linear Interpolation)	$Y = FUNCT(X)$
$Y = RNDGEN(P)$ $P = ANY$ ODD INTEGER NOISE(RANDOM NUMBER) GENER- ATOR WITH A UNIFORM DISTRIBUTION	UNIFORM DISTRIBUTION OF VARIABLE Y $p(Y)$ = Probability distri- bution Function:

TABLE IV

AIRCRAFT STATE EQUATIONS MATRICES

[A]

$$
\begin{bmatrix}
X_u & X_w & -g & 0 \\
\dfrac{Z_u}{1-Z_{\dot{w}}} & \dfrac{Z_w}{1-Z_{\dot{w}}} & 0 & U_0 \\
0 & 0 & 0 & 1.0 \\
M_u + \dfrac{M_{\dot{w}} Z_u}{1-Z_{\dot{w}}} & M_w + \dfrac{M_{\dot{w}} Z_w}{1-Z_{\dot{w}}} & 0 & M_q + \dfrac{M_{\dot{w}} U_0}{1-Z_{\dot{w}}}
\end{bmatrix}
$$

[B]

$$
\begin{bmatrix}
X_{\delta_e} & X_{\Delta T} & -X_u & -X_w \\
Z_{\delta_e} & Z_{\Delta T} & -Z_u & -Z_w \\
0 & 0 & 0 & 0 \\
M_{\delta_e} + \dfrac{M_{\dot{w}} Z_{\delta_e}}{1-Z_{\dot{w}}} & M_{\Delta T} + \dfrac{M_{\dot{w}} Z_{\Delta T}}{1-Z_{\dot{w}}} & -M_u - \dfrac{M_{\dot{w}} Z_u}{1-Z_{\dot{w}}} & -M_w - \dfrac{M_{\dot{w}} Z_w}{1-Z_{\dot{w}}}
\end{bmatrix}
$$

TABLE IV (continued)

[C]

$$
\begin{bmatrix}
0 & -1.0 & U_0 & 0 \\[2em]
\dfrac{Z_u}{1-Z_{\dot{w}}} & Z_w & 0 & 0 \\[2em]
-1'_x\left(M_u + \dfrac{M_w Z_u}{1-Z_{\dot{w}}}\right) & -1_x\left(M_w + \dfrac{M_{\dot{w}} Z_w}{1-Z_{\dot{w}}}\right) & 0 & -1_x\left(M_q + \dfrac{M_{\dot{w}} U_0}{1-Z_{\dot{w}}}\right)
\end{bmatrix}
$$

[D]

$$
\begin{bmatrix}
0 & 0 & 0 & 0 \\[2em]
Z_{\delta_e} & Z_{\Delta T} & -Z_u & -Z_w \\[2em]
-1_x\left(M_{\delta_e} + \dfrac{M_{\dot{w}} Z_{\delta_e}}{1-Z_{\dot{w}}}\right) & -1_x\left(M_{\Delta T} + \dfrac{M_{\dot{w}} Z_{\Delta T}}{1-Z_{\dot{w}}}\right) & 1_x\left(M_u + \dfrac{M_{\dot{w}} Z_u}{1-Z_{\dot{w}}}\right) & 1_x\left(M_w + \dfrac{M_{\dot{w}} Z_w}{1-Z_{\dot{w}}}\right)
\end{bmatrix}
$$

[E]

$$
\begin{bmatrix}
0 & 0 & 0 \\[1em]
0 & 0 & 0 \\[1em]
0 & 1.0 & 0
\end{bmatrix}
$$

TABLE   V

AIRCRAFT OPEN LOOP TRANSFER FUNCTION

NUMERATORS AND DENOMINATOR

$$\Delta \quad = \quad s^4 + 0.973939s^3 + 1.97797s^2 + 0.109846s + 0.070689$$

$$N^w_{\Delta T} \quad = - \ 0.00025s^3 + 0.0003986s^2 - 0.0001281s + 0.00003824$$

$$N^\theta_{\Delta T} \quad = \quad 0.00000407s^2 + 0.00000422s + 0.00000320s$$

$$N^u_{\Delta T} \quad = \quad 0.001317s^3 + 0.001195s^2 + 0.002435s - 0.0001321$$

$$N^w_{\delta_e} \quad = - \ 14.7135s^3 - 483.007s^2 - 26.3803s - 20.1217$$

$$N^u_{\delta_e} \quad = \quad 0.732836s^3 - 0.272704s^2 + 40.6515s + 33.4610$$

$$N^u_{u_g} \quad = \quad 0.054534s^3 + 0.0685976s^2 + 0.109846s + 0.070689$$

$$N^{u \ w}_{\delta_e \Delta T} \quad = \quad 0.0191945s^2 + 0.635365s - 0.0194913$$

$$N^{u \ \theta}_{\delta_e \Delta T} \quad = \quad 0.00288013s + 0.0013343$$

$$N^{w \ u}_{\delta_e \Delta T} \quad = - \ 0.0191945s^2 - 0.635365s + 0.0194913$$

$$N^{w \ \theta}_{\delta_e \Delta T} \quad = - \ 0.00060607s - 0.00085794$$

$$N^{u \ w}_{u_g \Delta T} \quad = - \ 0.00039155s^2 - 0.00012806s + 0.00003824$$

$$N^{u \ \theta}_{u_g \Delta T} \quad = \quad 0.0000001131s + 0.00000320$$

TABLE VI

AIRCRAFT TRANSFER FUNCTION NUMERATORS AND

DENOMINATOR FOR STANDARD APCS LOOP CLOSURES

T_e = 1.8 SECONDS

$$\Delta'' = \frac{1}{s(s+1)(s+2.857)(s+0.56)} \left\{ [0.303,0.278](-0.263) \right.$$

$$\left. (0.032)(-1.099)[0.346,1.44](-2.89) \right\}$$

$$N_{\delta_e}^{u} \bigg]_{std} = \frac{0.7328}{s(s+1)(s+2.857)(s+0.435)(s+0.56)} \left\{ [0.504,0.182] \right.$$

$$\left. (0.150)[-0.176,1.38](-0.807)(-3.41)(49.5) \right\}$$

$$N_{\delta_e}^{w} \bigg]_{std} = \frac{-14.71}{(s+1)(s+0.435)(s+0.56)} \left\{ [0.389,0.257](-0.253) \right.$$

$$\left. (-0.584)(-1.05)(-32.2) \right\}$$

$$N_{u_g}^{u} \bigg]_{std} = \frac{0.5453}{s(s+1)(s+2.857)(s+0.56)} \left\{ [0.308,0.716](0.00948) \right.$$

$$\left. [0.0836,1.74](-1.58)(-3.37) \right\}$$

Notation: $[\zeta, \omega_n]$ represents $(s^2+2\zeta\omega_n+\omega_n^2)$

(τ) represents $(s-\tau)$

positive ζ and negative τ represent stable roots

TABLE VII
RMS VELOCITY ERROR SUMMARY

APCS Configuration	$u_0=5$ $w_0=-5$	$u_0=-5$ $w_0=5$	$Z_{e_0}=10$	$Z_{e_0}=-10$	$\bar{w}_g=5$	$\bar{u}_g=5$
Standard	3.09	2.87	3.14	3.06	7.40	6.26
Long Accel $K_{\dot{u}}=1.0$	3.02	2.85	3.08	3.03	7.01	5.63
$=2.0$	3.03	2.91	3.05	3.01	6.75	5.28
$=3.0$	3.09	3.00	3.03	2.96	6.57	5.05
Long Veloc $K_u=1.0'$	2.78	2.57	3.09	3.05	7.11	4.16
$=2.0$	2.69	2.38	3.05	3.03	6.72	3.44
$=3.0$	2.59	2.20	3.01	3.01	6.40	3.28
Prop+Int u $K_u(u+\frac{1}{2}\int u)$ $K_u=1.0$	3.26	2.95	3.16	3.11	7.79	4.46
$=3.0$	3.88	3.05	3.10	3.11	6.23	3.30
Prop+Accel u $K_{\dot{u}}(\dot{u}+K_q u)$ $K_q=1.0$ $K_{\dot{u}}=1.0$	2.65	2.48	3.05	3.02	6.76	4.07
$=3.0$	2.35	2.30	2.99	2.98	6.18	3.55
$K_q=0.5$ $K_{\dot{u}}=1.0$	2.75	2.60	3.07	3.02	6.87	4.61
$=2.0*$	2.61	2.48	3.03	3.00	6.55	4.06
$=3.0$	2.52	2.41	3.01	2.96	6.35	3.84
$K_q=0.2$ $K_{\dot{u}}=1.0$	2.88	2.72	3.07	3.03	6.94	5.12
$=3.0$	2.73	2.64	3.02	2.99	6.46	4.33

* Underlined values denote revised configuration.

TABLE VIII

AIRCRAFT TRANSFER FUNCTIONS FOR STANDARD AND REVISED

APCS CLOSURES; T_e = 1.8 SECONDS

$$\frac{u}{\delta_e}(s)_{std} = \frac{0.733[0.504,0.182](0.150)(-0.807)[-0.176,1.38](-3.41)(49.5)}{(-0.435)[0.303,0.278](-0.263)(0.0320)(-1.099)[0.346,1.44](-2.89)}$$

$$\frac{u}{\delta_e}(s)_{rev} = \frac{0.733[0.504,0.182](0.150)(-0.807)[-0.176,1.38](-3.41)(49.5)}{(-0.435)[0.764,0.514](-0.0630)(0.0320)(-1.15)(0.0372)[0.361,1.44](-2.90)}$$

$$\frac{w}{\delta_e}(s)_{std} = \frac{-14.7(-0.253)[0.389,0.257](-0.584)(-1.05)(-32.3)(0.0)(-2.857)}{(-0.435)[0.303,0.278](-0.263)(0.0320)(-1.099)[0.346,1.44](-2.89)}$$

$$\frac{w}{\delta_e}(s)_{rev} = \frac{-14.7(-0.660)[0.880,0.458](-0.0447)(-1.094)(-32.2)(0.0)(-2.857)}{(-0.435)[0.764,0.514](-0.0630)(-1.15)(0.0372)[0.361,1.44](-2.90)}$$

$$\frac{u}{u_g}(s)_{std} = \frac{0.0545[0.308,0.716](0.00948)[0.0836,1.74](-1.58)(-3.37)}{[0.303,0.278](-0.263)(0.0320)(-1.099)[0.346,1.44](-2.89)}$$

$$\frac{u}{u_g}(s)_{rev} = \frac{0.0545[0.308,0.716](0.00948)[0.0836,1.74](-1.58)(-3.37)}{[0.764,0.514](-0.0630)(-1.15)(0.0372)[0.361,1.44](-2.90)}$$

Notation: $[\zeta, \omega_n]$ represents $(s^2 + 2\zeta\omega_n s + \omega_n^2)$; (τ) represents $(s-\tau)$; positive ζ and negative τ represent stable roots.

43

$$
\begin{bmatrix}
s-X_u & -X_w & g & 0 & 0 & 0 \\
-Z_u & (1-Z_{\dot{w}})s-Z_w & -U_0 s & 0 & 0 & 0 \\
-M_u & -(M_{\dot{w}}s+M_w) & s^2-M_q s & 0 & 0 & 0 \\
0 & 1 & -U_0 & 1 & 0 & 0 \\
0 & -s & U_0 s & 0 & 1 & 0 \\
0 & -s & 1_x s^2+U_0 s & 0 & 0 & 1
\end{bmatrix}
\begin{bmatrix}
u \\ w \\ \theta \\ \dot{h} \\ a_z \\ a'_z
\end{bmatrix}
=
\begin{bmatrix}
X_{\delta_e} & X_{\Delta T} & -X_u & -X_w \\
Z_{\delta_e} & Z_{\Delta T} & -Z_u & -Z_w \\
M_{\delta_e} & M_{\Delta T} & -M_u & -M_w \\
0 & 0 & 0 & 0 \\
0 & 0 & 0 & 0 \\
0 & 0 & 0 & 0
\end{bmatrix}
\begin{bmatrix}
\delta_e \\ \Delta T \\ u_g \\ w_g
\end{bmatrix}
$$

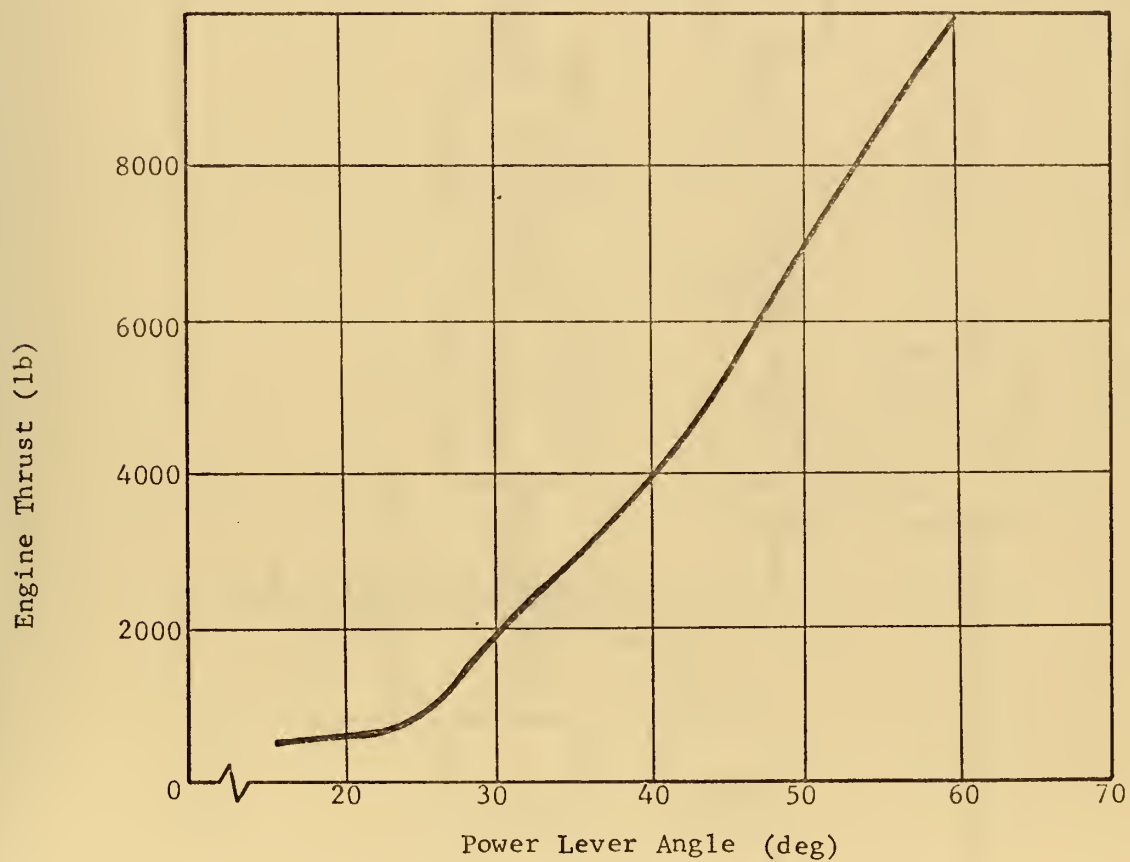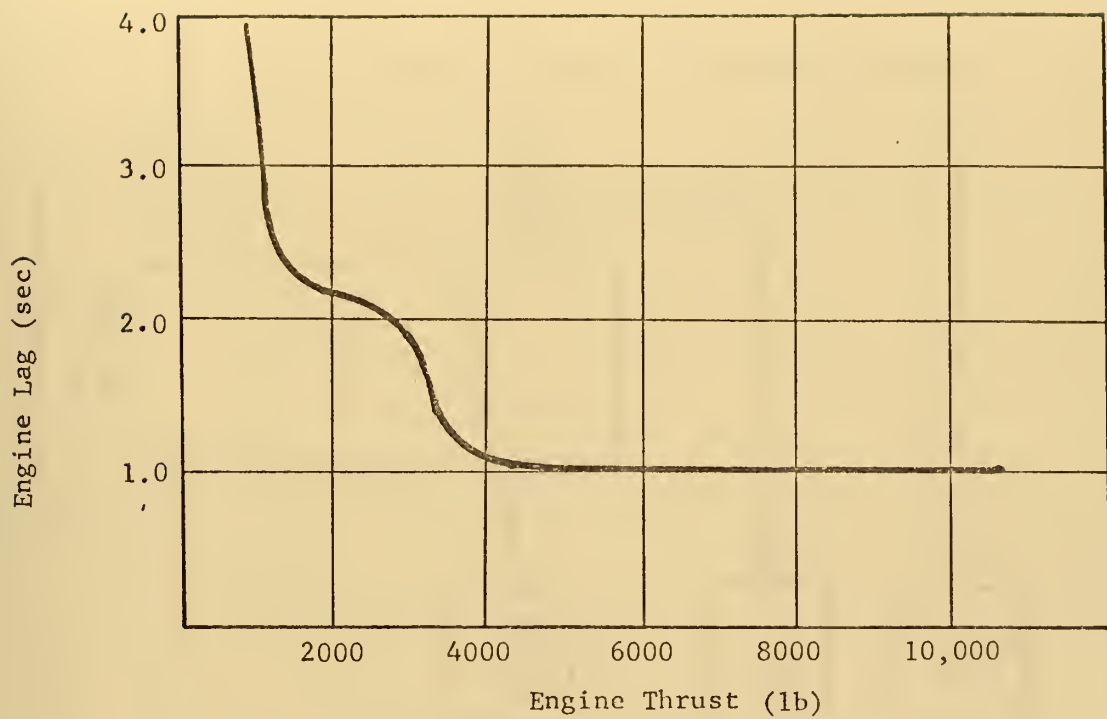FIGURE 1. AIRCRAFT EQUATIONS OF MOTION
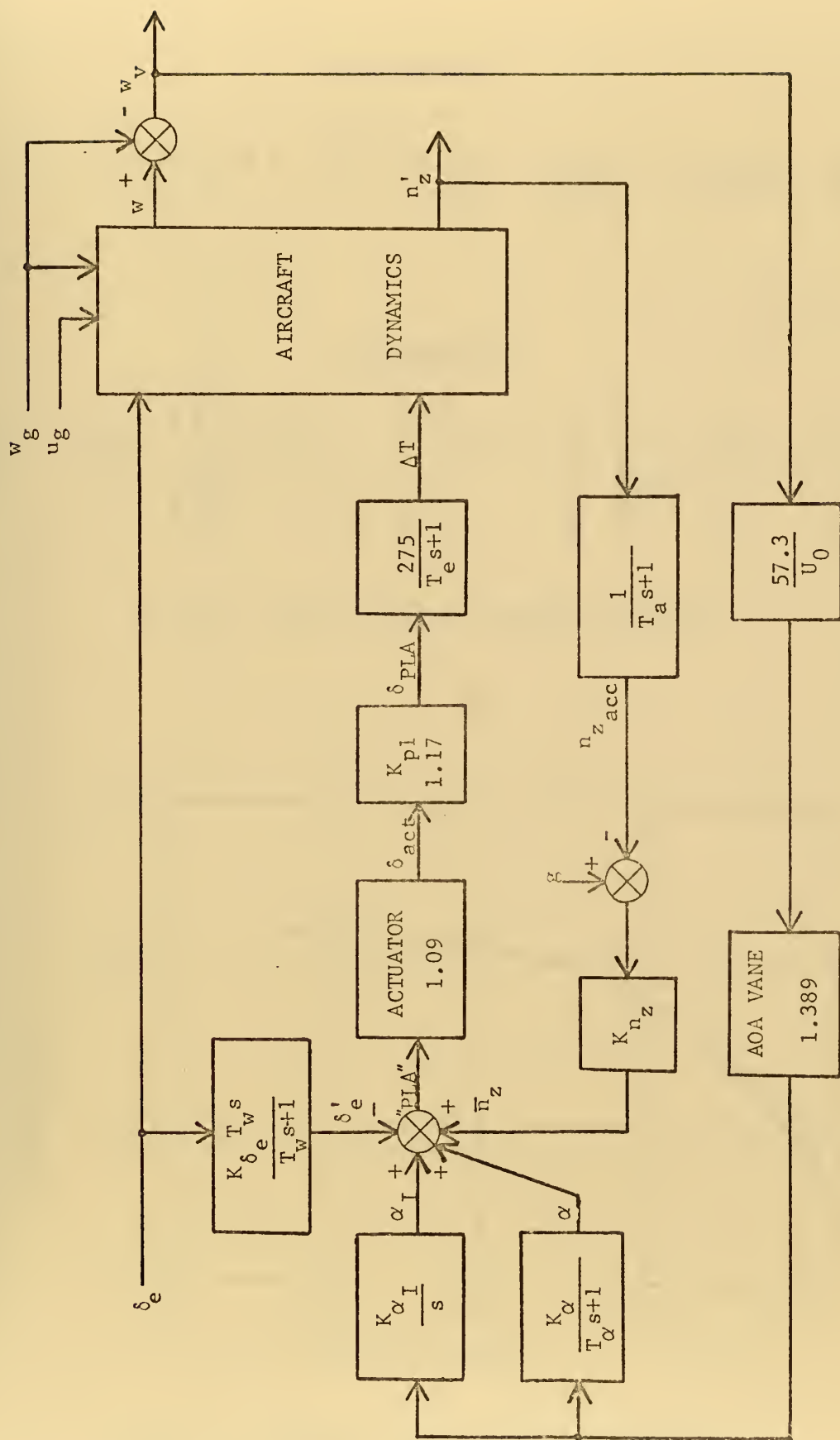
FIGURE 2. TF41-A-2 ENGINE CHARACTERISTICS

FIGURE 3. STANDARD APCS BLOCK DIAGRAM

46

$$\delta_e = \left[K_\theta(\theta - \theta_c) + K_{\dot\theta}\dot\theta + \frac{K_{n_z} N_z}{0.55s + 1} \right] \left[\frac{1}{\left(\frac{s}{20} + 1\right)\left[\left(\frac{s}{20}\right)^2 + \frac{2(0.7)s}{20} + 1\right]} \right]$$

ACLS EQUATION

$$\frac{\theta_c}{Z_e} = \frac{K_c K_x}{K_p s + 1} \left\{ \left[\frac{\frac{s}{3.9} + 1}{\left(\frac{s}{5}\right)^2 + \frac{s}{3.5} + 1} \right] \left[\frac{t_i K_x}{s} + 1 \right] + \left[\frac{R_x s}{\left(\frac{s}{5}\right)^2 + \frac{s}{3.5} + 1} \right] t_r \right\}$$
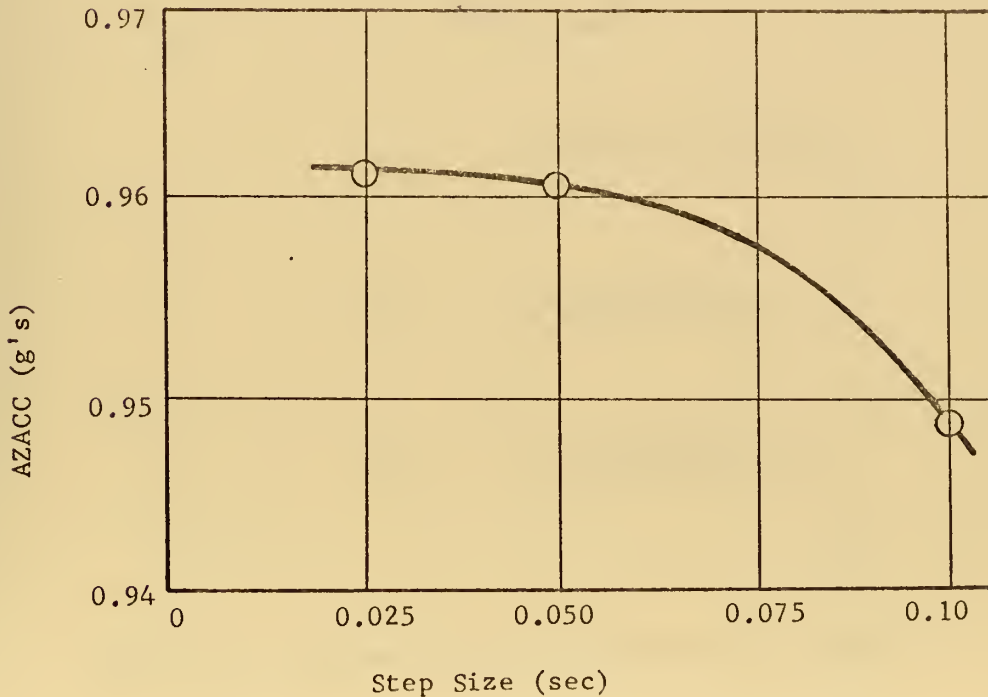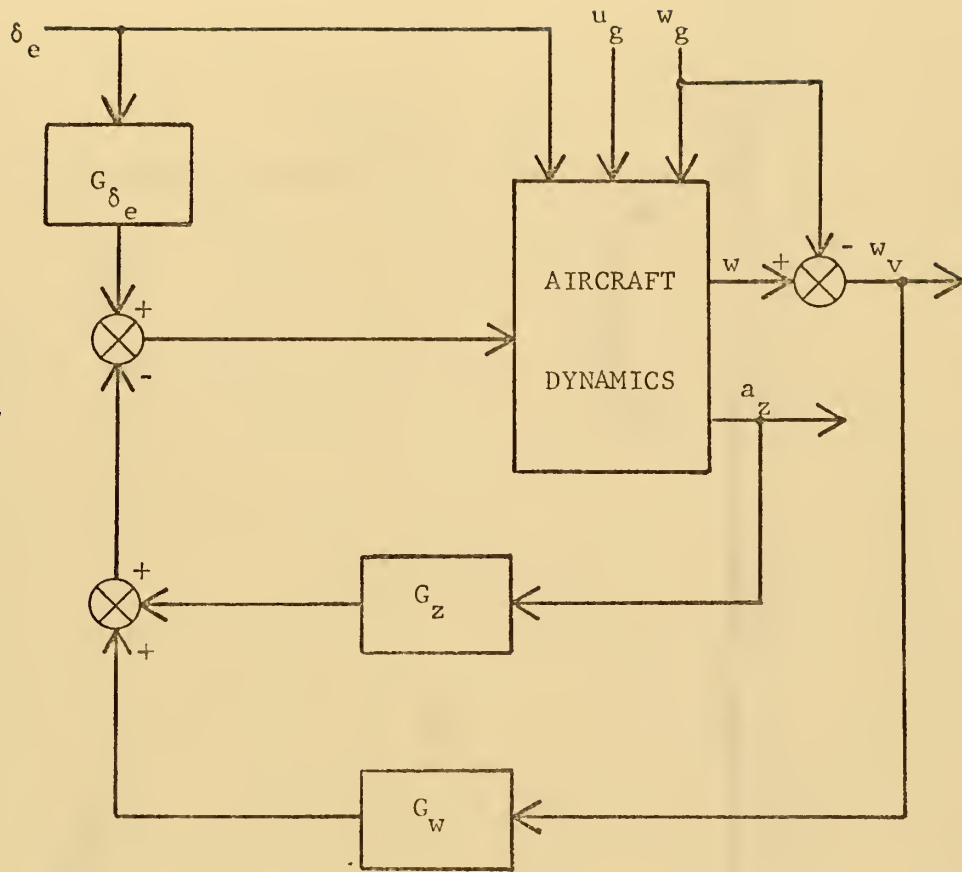
FIGURE 4. AFCS AND ACLS TRANSFER FUNCTIONS

FIGURE 5. NUMERICAL INTEGRATION ERROR ANALYSIS

$$G_w = - \frac{1021.5(s+0.197)}{T_e s(s+2.857)(s+1/T_e)}$$

$$G_z = - \frac{327.2}{T_e(s+1)(s+1/T_e)}$$

$$G_{\delta_e} \doteq - \frac{50,235s}{T_e(s+0.435)(s+1/T_e)}$$

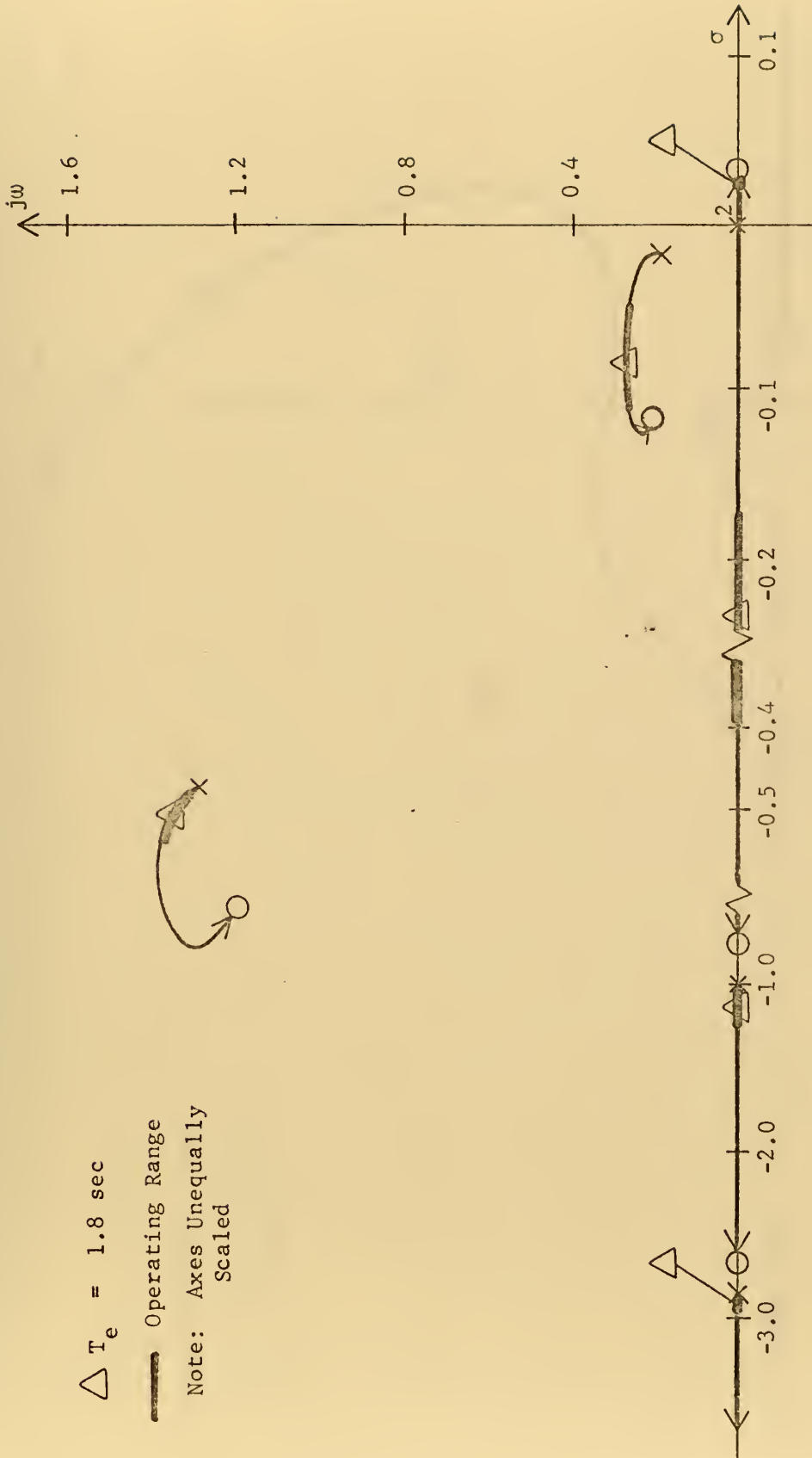FIGURE 6. STANDARD APCS EQUIVALENT BLOCK DIAGRAM

48

FIGURE 7. LOCI OF ZEROES OF Δ' FOR $1/T_e$ VARIATION

$\triangle T_e$ = 1.8 sec

━━ Operating Range

Note: Axes Unequally
Scaled

49
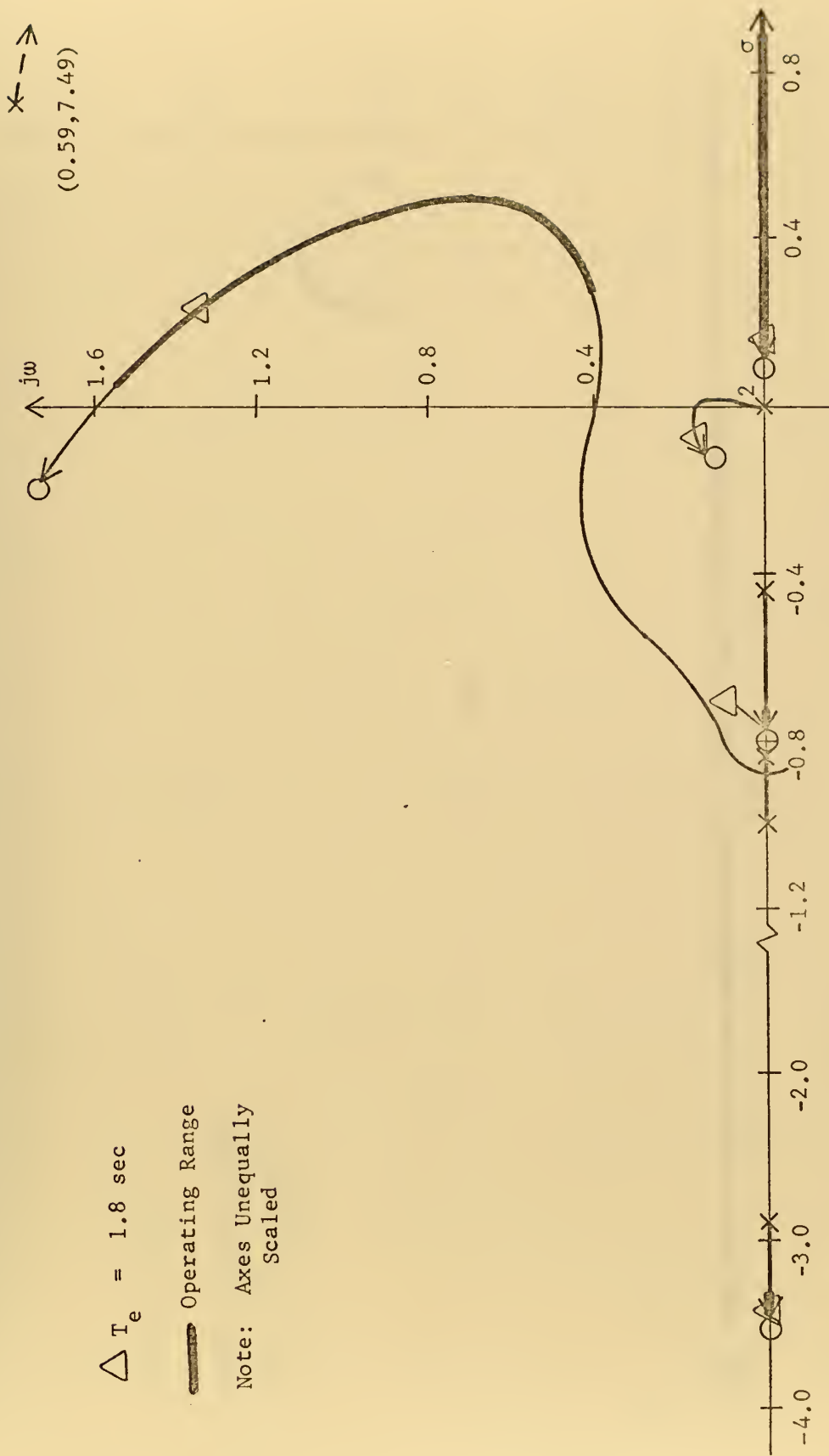
FIGURE 8. LOCI OF ZEROES OF $N_{\delta_e}^u \Big]_{std}$ FOR $1/T_e$ VARIATION

$\triangle \tau_e = 1.8$ sec

$(0.59, 7.49)$

$\quad\quad$ Operating Range

Note: Axes Unequally
$\quad\quad\quad$ Scaled

jw

σ

50
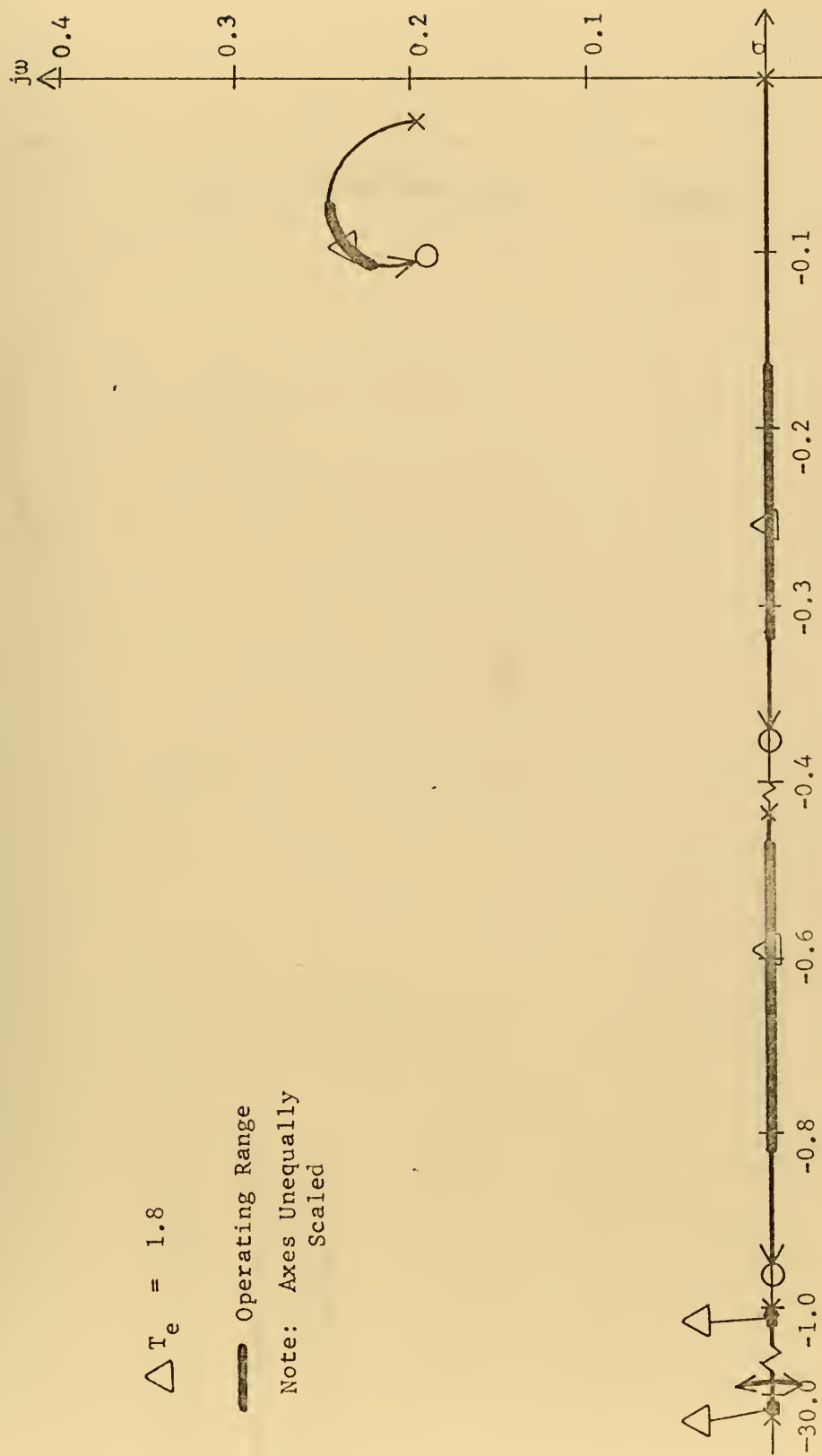
FIGURE 9. LOCI OF ZEROES OF $N_{\delta_e}^w \Big]_{std}$ FOR $1/T_e$ VARIATION

$\triangle T_e = 1.8$

■■■ Operating Range

Note: Axes Unequally Scaled

51

FIGURE 10. LOCI OF ZEROES OF $N_u^u \rfloor_{std}$ FOR $1/T_e$ VARIATION

$\triangle$ T_e = 1.8 sec

━━━ Operating Range

Note: Axes Unequally
      Scaled

52
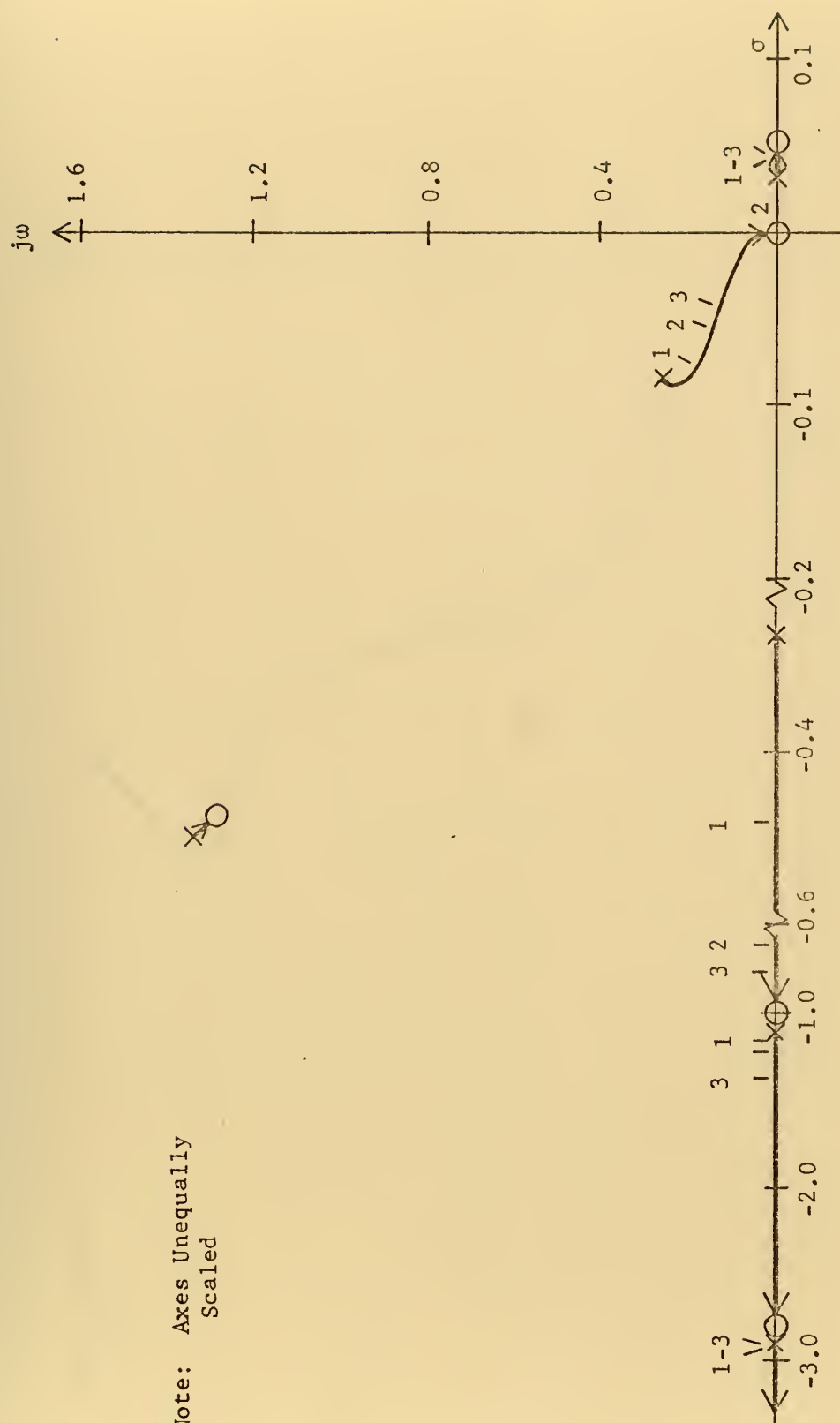
FIGURE 11. LOCI OF ZEROES OF Δ''' FOR $K_u^{\bullet}$ VARIATION

Note: Axes Unequally Scaled

53

Note: Axes Unequally Scaled
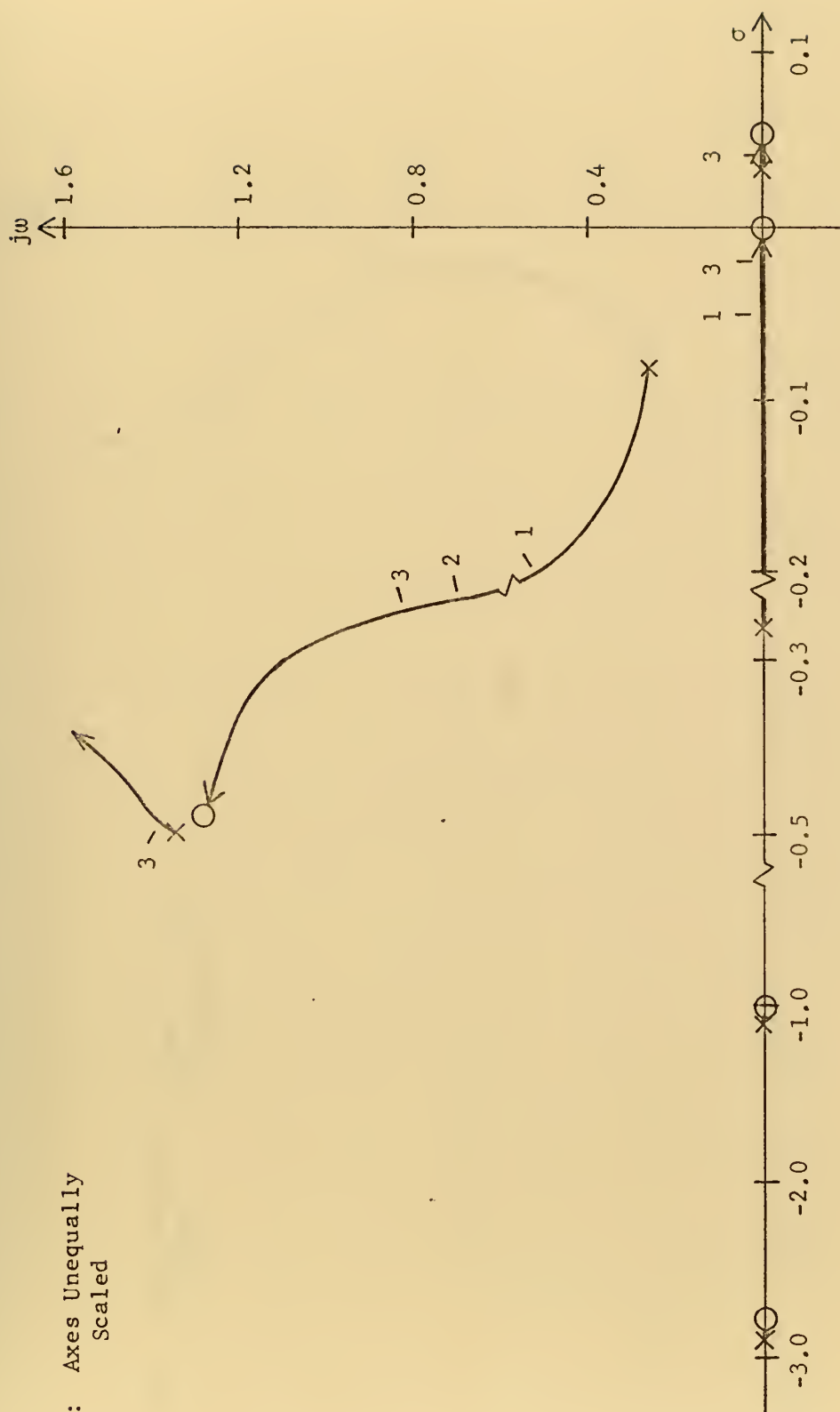
FIGURE 12. LOCI OF ZEROES OF Δ''' FOR K_u VARIATION

54
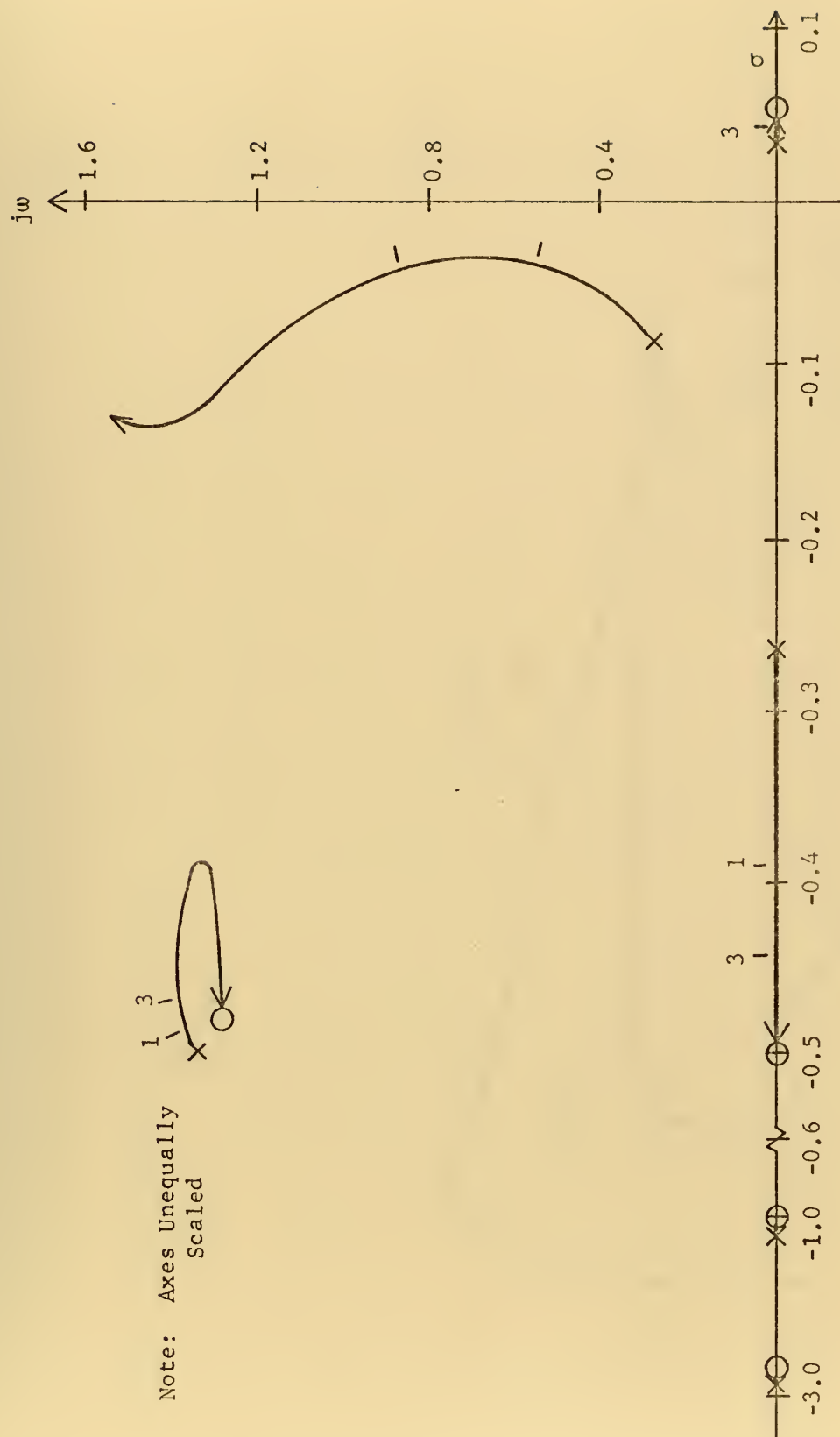
FIGURE 13. LOCI OF ZEROES OF Δ''' FOR K_u VARIATION; $K_p = 0.5$
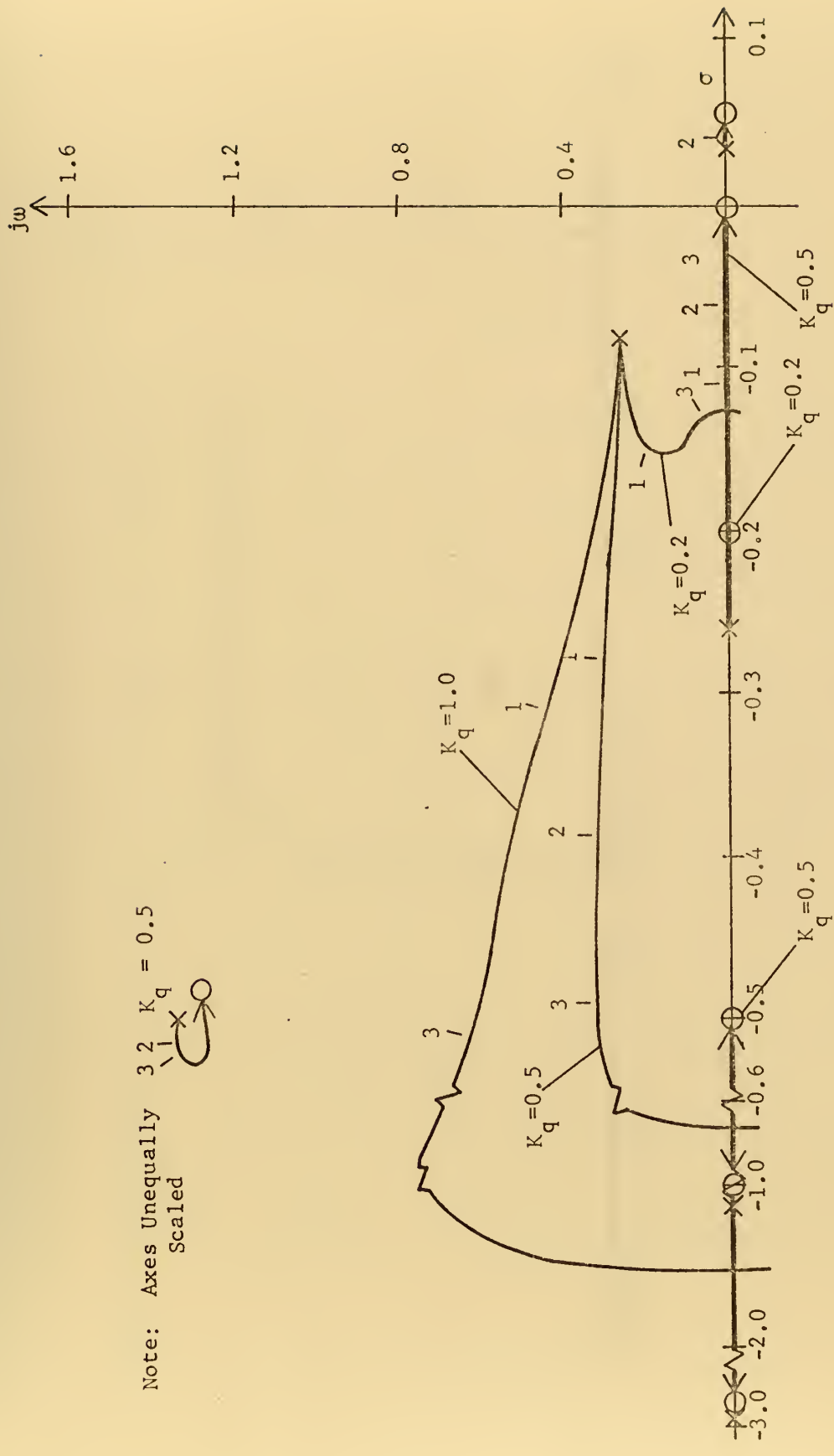
FIGURE 14. LOCI OF ZEROES OF Δ''' FOR $K_u^{\bullet}$ VARIATION; K_q=0.2,0.5,1.0
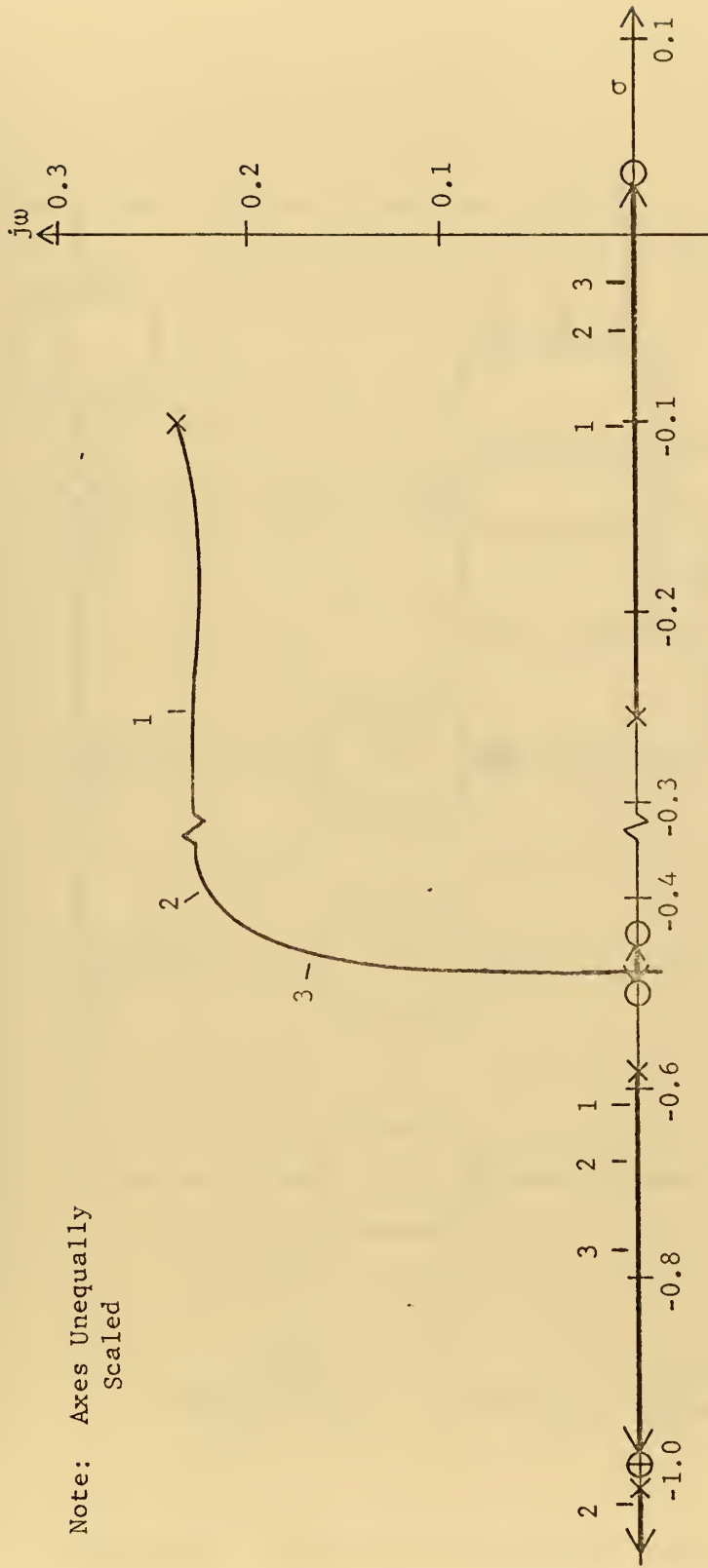
FIGURE 15. LOCI OF ZEROES OF $N_{\delta_e}^w$ FOR $K_u^{\cdot}$ VARIATION; $K_q = 0.5$
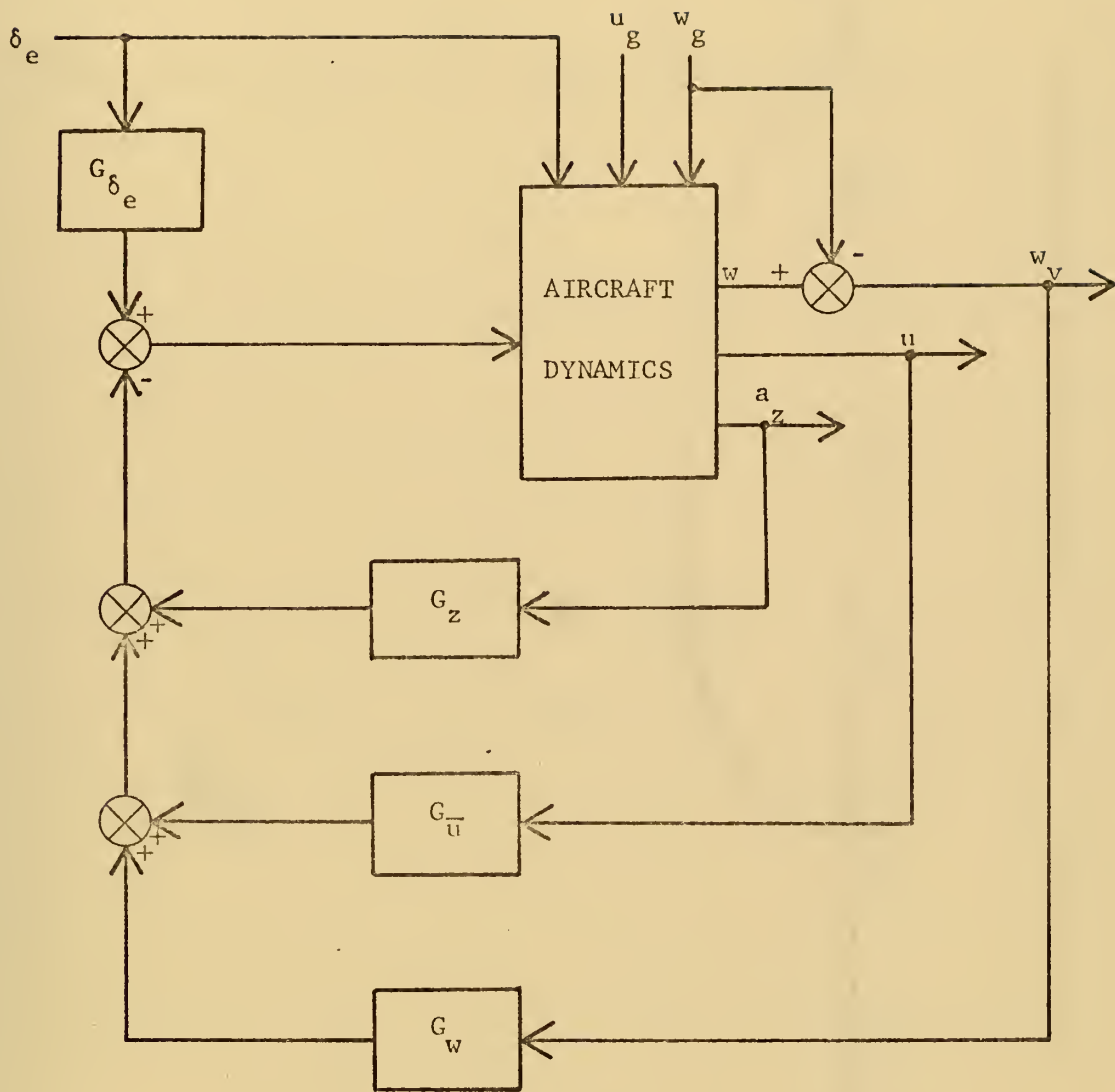
$$G_{\overline{u}} = \frac{350.7}{T_e(s+1/T_e)} \cdot K_{\dot{u}} (s+K_q) = \frac{701.4(s+0.5)}{T_e(s+1/T_e)}$$

FIGURE 16.   REVISED APCS EQUIVALENT BLOCK DIAGRAM

FIGURE 17. LOCI OF ZEROES Δ''' FOR $1/T_e$ VARIATION; REVISED CONFIGURATION

$\triangle$ T_e = 1.8 sec

—— Operating Range

Note: Axes Unequally
         Scaled
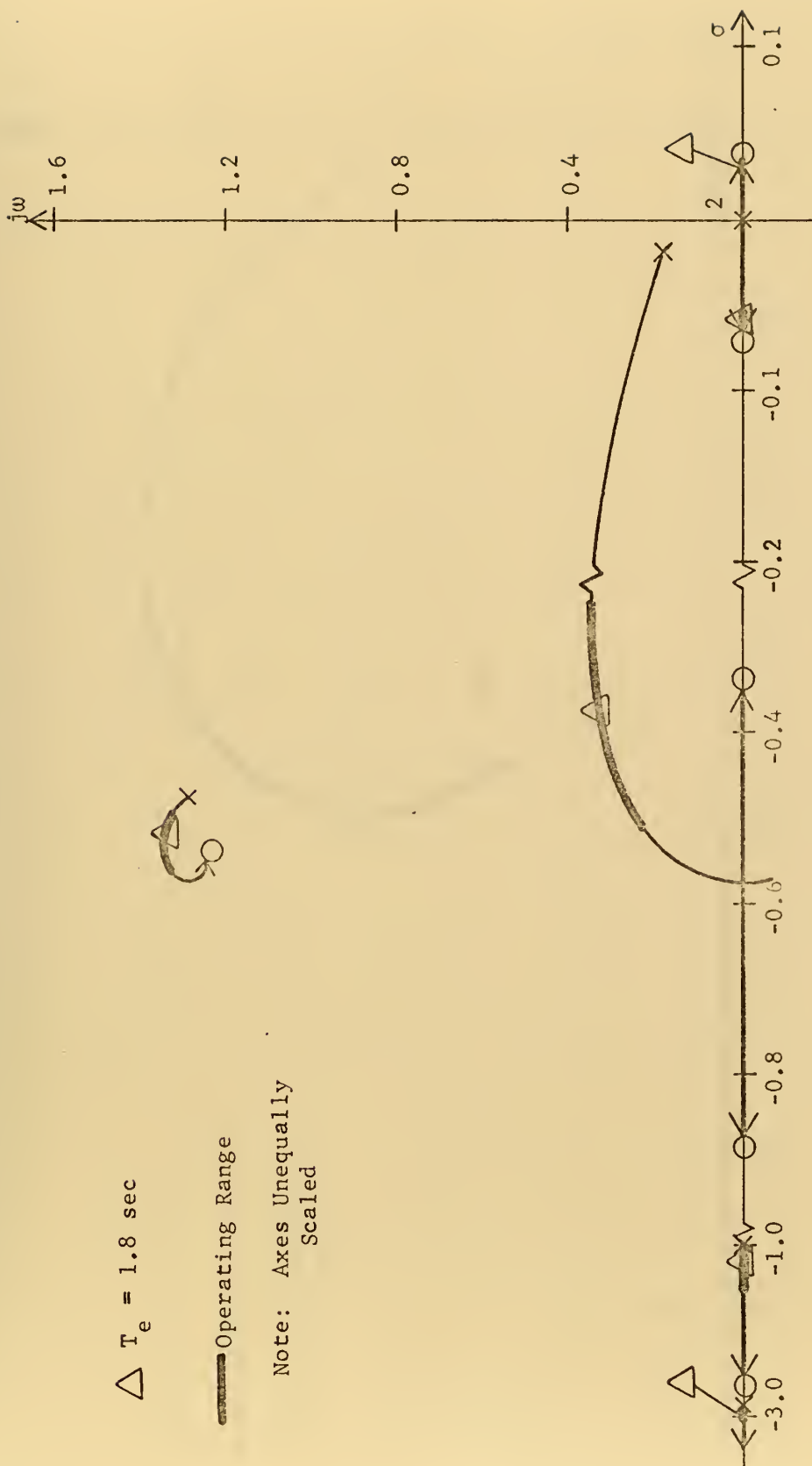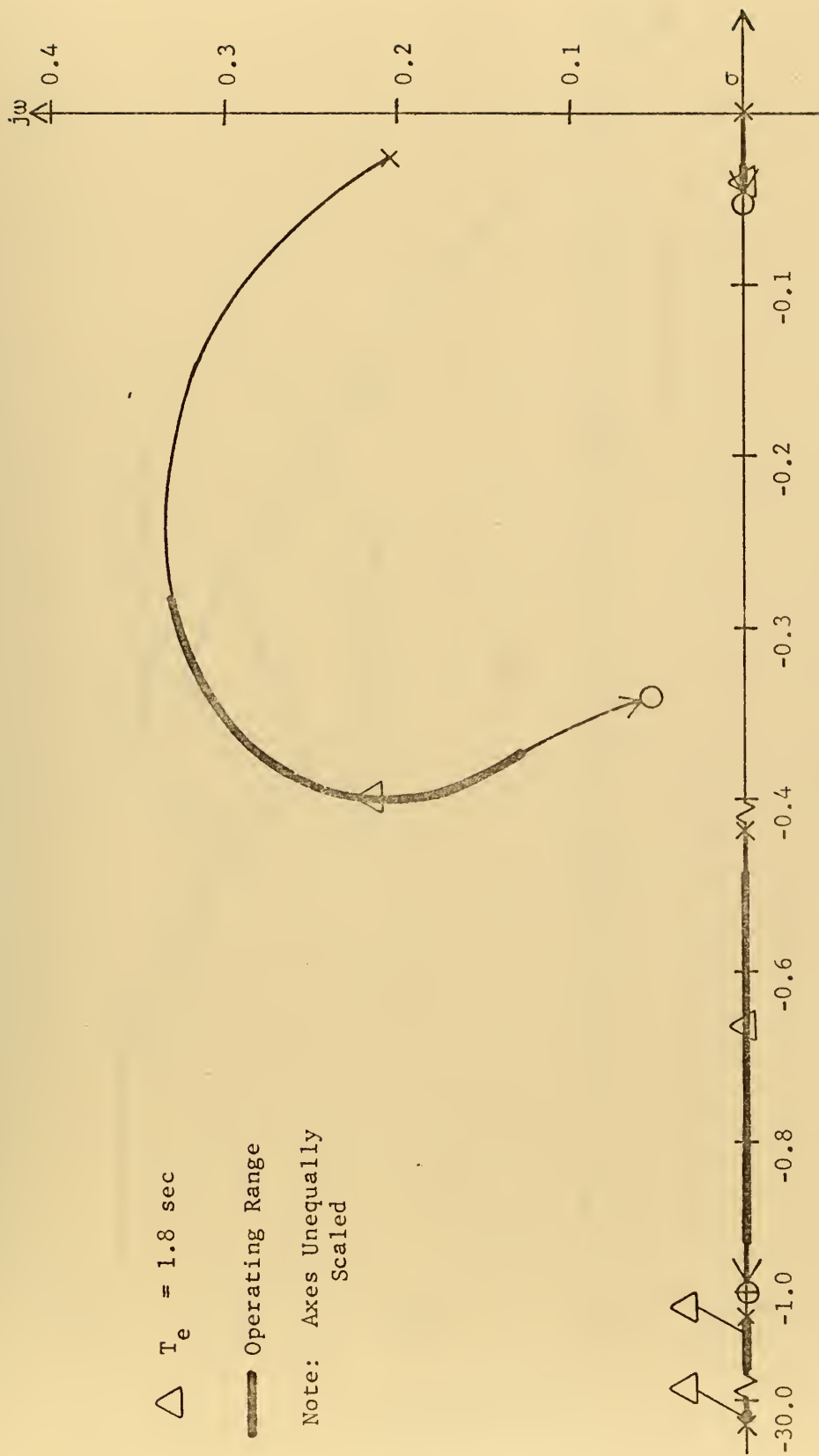
FIGURE 18. LOCI OF ZEROES OF $N_{\delta_e}^w$] FOR $1/T_e$ VARIATION; REVISED CONFIGURATION rev

$\triangle$ T_e = 1.8 sec

▬ Operating Range

Note: Axes Unequally Scaled
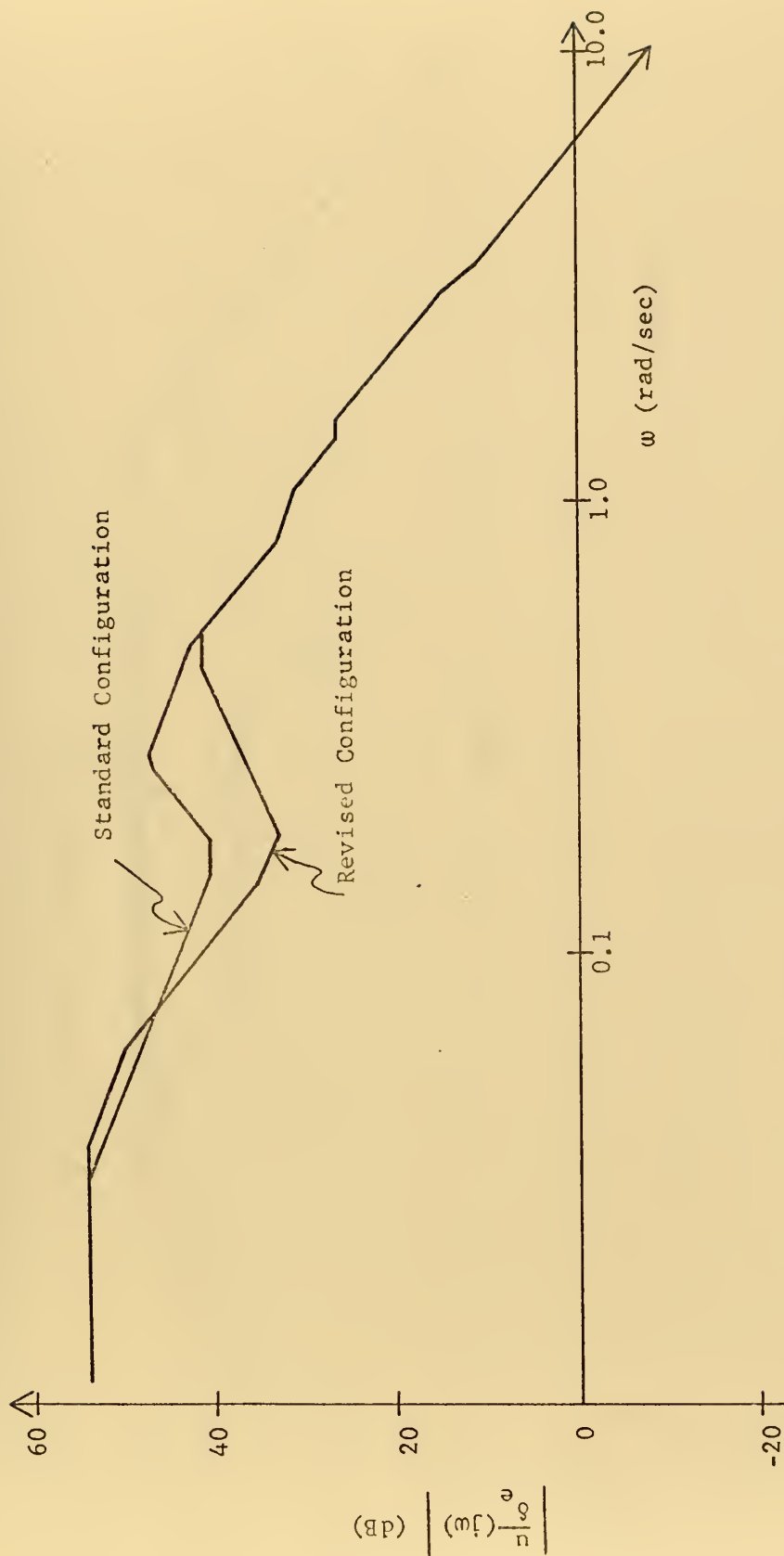
FIGURE 19. AIRSPEED REPSONSE TO ELEVATOR, BODE PLOT

61
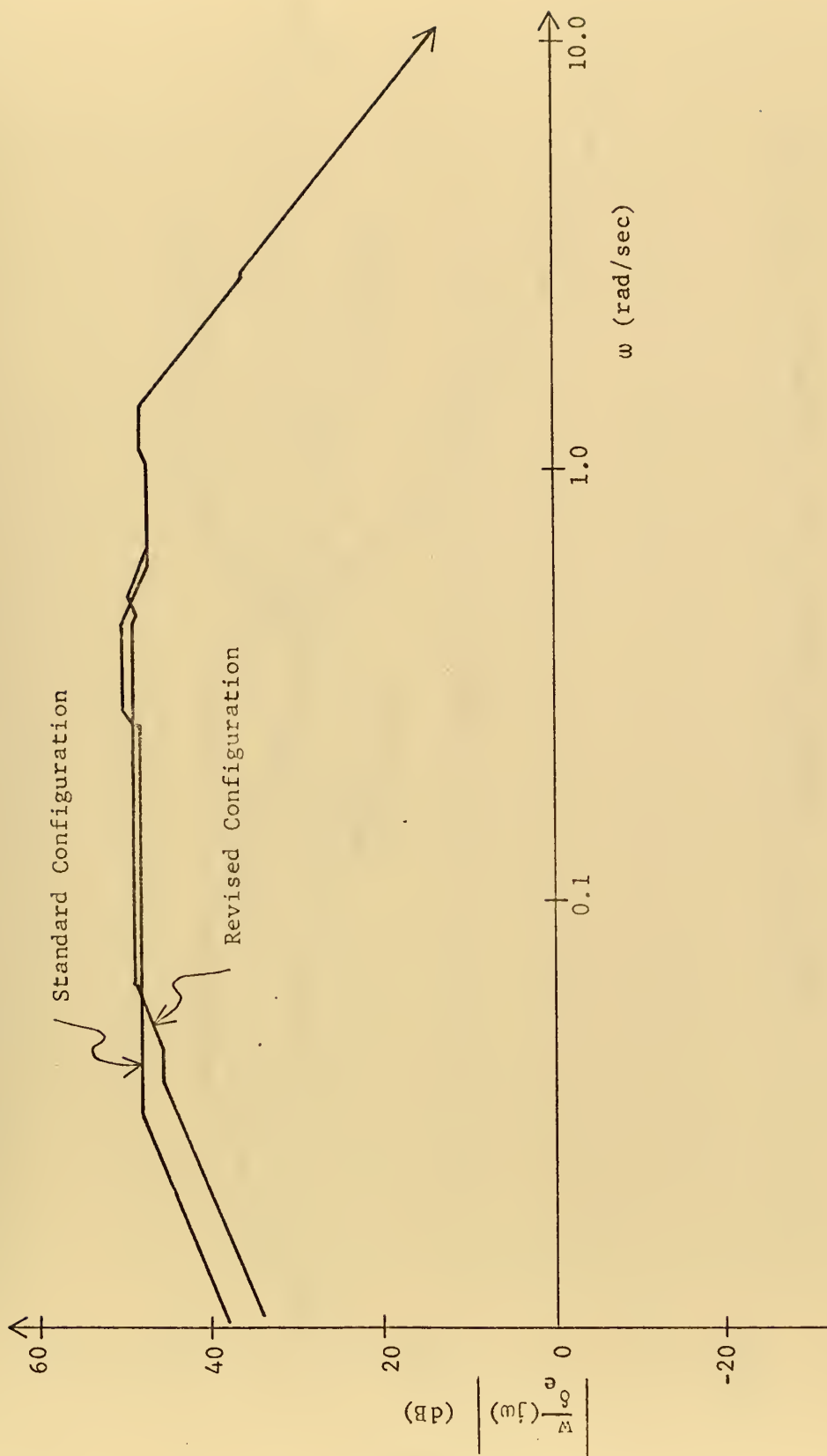
FIGURE 20. ANGLE OF ATTACK RESPONSE TO ELEVATOR, BODE PLOT

62
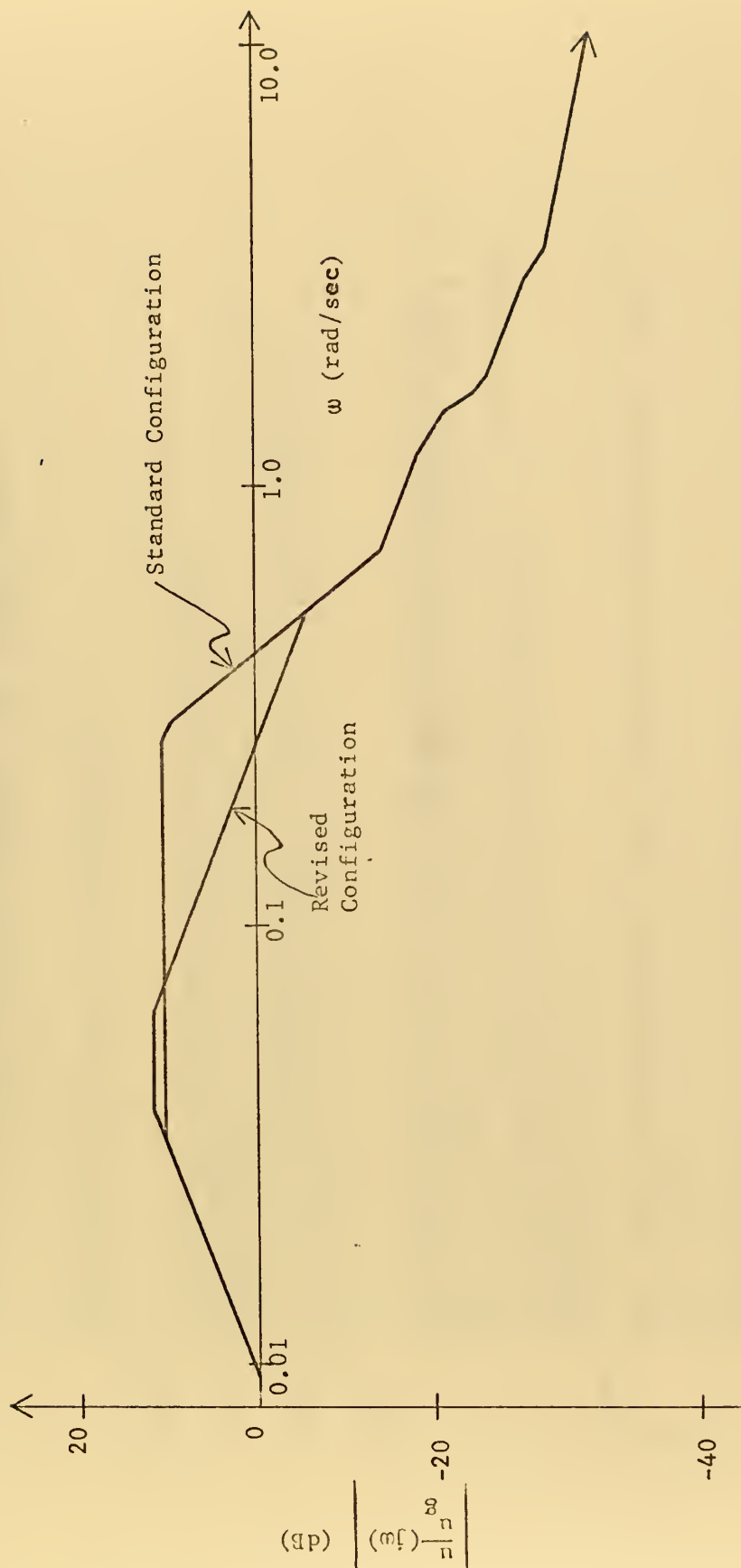
FIGURE 21. AIRSPEED RESPONSE TO LONGITUDINAL GUST, BODE PLOT

63

CSMP COMPUTER PROGRAM AND SAMPLE OUTPUT

```
/        DIMENSION A(4,4),B(4,4),C(3,4),D(3,4)
INITIAL  FIXED I,J
NOSORT
         READ(5,100) ((A(I,J),J=1,4),I=1,4),((B(I,J),J=1,4),I=1,4),
        (((C(I,J),J=1,4),I=1,3),((D(I,J),J=1,4),I=1,3)
100      FORMAT(4F10.6)
         WRITE(6,1000) ((A(I,J),J=1,4),(B(I,J),J=1,4),I=1,4),((C(I,J),
        J=1,4),(D(I,J),J=1,4),I=1,3)
1000     FORMAT(//T35,'A-MATRIX',T99,'B-MATRIX'//4(T06,4F15.6,T71,
        $4F15.6/)/T35,'C-MATRIX',T99,'D-MATRIX'//3(T06,4F15.6,T71,
        $4F15.6/)/)
SORT

FUNCTION TECURV=-2100.0,-0.4,0.,-1800.0,0.2,-5.,-1500.0,2.,-5.,-1200.0,
2.18,-800.0,2.13,-400.0,2.08,-200.0,2.03,-0.,1.85,200.0,1.55,
400.0,1.27,600.0,1.15,800.0,1.,1200.0,1.,1200.0,1.,05,2000.0,1.0,3000.0,
1.0
PARAM A0=0.0242,A1=0.369,B0=66.489,B1=43.989,B2=9.7996,K=0.5923
INCON X10=0.0,X20=0.0,X30=0.0,X40=0.0,ZE0=0.0
CONSTANT KP=0.5,KUDOT=2.0
WGUST=0.0
DYNAMIC
* * * * *  APCS INCLUDES PROPORTIONSL PLUS DERIVATIVE LONGITUDINAL VELOCITY

* * *  GUST INPUT
RAND=385.0*(RNDGEN(3)-0.5)
UGUST=CMPXPL(0.0,0.0,0.707,1.0,RAND)
UG=UGUST**2
UGMSV=INTGRL(0.0,UG)

AIRCRAFT EQUATIONS OF MOTION
XTEMP1=A(1,1)*X1+A(1,2)*X2+A(1,3)*X3+A(1,4)*X4+B(1,1)*ELEV
+B(1,2)*THRUST+B(1,3)*UGUST+B(1,4)*WGUST
X1=INTGRL(X10,XTEMP1)
XTEMP2=A(2,1)*X1+A(2,2)*X2+A(2,3)*X3+A(2,4)*X4+B(2,1)*ELEV
+B(2,2)*THRUST+B(2,3)*UGUST+B(2,4)*WGUST
```

```
X2=INTGRL(X20,XTEMP2)
X3=INTGRL(X30,X4)
XTEMP4=A(4,1)*X1+A(4,2)*X2+A(4,3)*X3+A(4,4)*X4+B(4,1)*ELEV
+B(4,2)*THRUST+B(4,3)*UGUST+B(4,4)*WGUST
X4=INTGRL(X40,XTEMP4)
HCOT =C(1,1)*X1+C(1,2)*X2+C(1,3)*X3+C(1,4)*X4
AZ   =C(2,1)*X1+C(2,2)*X2+C(2,3)*X3+C(2,4)*X4+D(2,1)*ELEV
+D(2,2)*THRUST+D(2,3)*UGUST+D(2,4)*WGUST
AZPRIM=C(3,1)*X1+C(3,2)*X2+C(3,3)*X3+C(3,4)*X4+D(3,1)*ELEV
+D(3,2)*THRUST+D(3,3)*UGUST+D(3,4)*WGUST+AZ

APCS EQUATIONS

ALPHAV=0.3651*(X2-WGUST)
ALPHAI=0.55*INTGRL(0.0,ALPHAV)
ALPHA=INTGRL(0.0,(2.6*ALPHAV-ALPHA)/0.35)
W1DOT=-0.435*W1+ELEV
W1=INTGRL(0.0,W1DOT)
ELEVP=143.2*W1DOT
NZP=1.0-0.03109*AZPRIM
NZACC=REALPL(1.0,-NZACC)
NZBAR=30.0*(1.0-NZACC)
TE=AFGEN(TECURV,THRUST)
PLA=NZBAR+ALPHA+ALPHAI-ELEVP-KUDOT*(XTEMP1+KP*X1)
THRUST=INTGRL(0.0,(350.7*PLA-THRUST)/TE)

ACLS EQUATIONS

ZF=INTGRL(ZEO,-HDOT)
ZI=K*INTGRL(0.0,ZE)
Y1=INTGRL(0.0,Y2)
Y2=INTGRL(0.0,Y3)
Y3DOT=-B0*Y1-B1*Y2-B2*Y3+ZI
Y3=INTGRL(0.0,Y3DOT)
THETAC=Y3+A1*Y2+A0*Y1

AFCS EQUATIONS

AZSTAR=REALPL(0.0,0.55;AZ)
ELEV=1.9*(X3-THETAC)+X4-0.00163*AZSTAR

VERTICAL AND HORIZONTAL VELOCITY ERROR

ERR1=X1**2
ERR2=X2**2
ERRCUM=INTGRL(0.0,ERR1+ERR2)

TIMER FINTIM=30.0,DELT=0.0500,OUTDEL=0.10,PRDEL=0.5
```

```
METHOD RKSFX
TITLE A-7E AIRCRAFT WITH APC/AFCS/ACL CLOSURES
PRINT ZE,THETA,ELEV,ELEVP,NZBAR,PLA,THRUST,ERRCUM
PREPARE X1,X2,ZE,THRUST,UGUST
TERMINAL
ERRRMS=SQRT(ERRCUM/30.0)
WRITE(6,2000) ERRRMS
2000 FORMAT(' 0',T10,'RMS VELOCITY ERROR=',F10.4///)
UGRMS=SQRT(UGMSV/30.0)
WRITE(6,3000) UGRMS
3000 FORMAT(' 0',T10,'RMS GUST LEVEL:',2F15.4///)
END
DATA
-0.05453      0.06433     -32.16        0.0
-0.7870      -0.5289        0.0        218.0
 0.0         -0.007811      0.0          1.0      0.3905
-0.000082    -0.001317      0.05453    -0.06433
-0.7328      -0.00025       0.28695      0.52887
-14.714      -0.000004      0.000082     0.0078.11
-2.1846      -1.0           218.0        0.0
-0.28695     -0.528887      0.0          2.61635
-0.00055      0.052334      0.0          0.52887
 0.0         -0.000025      0.28695      0.52887
-14.714      -0.000027     -0.00055     -0.052334
-14.6368
ENDDATA
STOP
ENDJOB
```

```
C      OFFLINE PLOTTING ROUTINE

       DIMENSION XOUT(6),X(900),U(900),V(900),W(900),Y(900),Z(900)
       REAL * 8 LABEL/8H         /,ITITLE(12)
       DATA ENDS/*END$*/
       DOUBLE PRECISION WORD

C      KGRAPH IS NO OF OUTPUT VARIABLES

       KGRAPH=6

C      READ CONSTANTS FOR DRAW

       READ(5,100) NOPLOT
   5   READ(5,100) NOCUR
 100   FORMAT((I2)
 200   READ(5,200)     (ITITLE(I),I=1,12)
       FORMAT(6A8)
 300   READ(5,300)   XSCL,YSCL,IUP,IRITE,MODEX,MODEY,IW,IHI,IGR
       FORMAT(9I5)
       IF(NOCUR-1)  55,10,15
  10   MODCUR=0
       GO TO 20
  15   MODCUR=1

C      READ DATA SET OF POINTS PRODUCED BY CSMP

  20   CONTINUE

C      READ 10 INTRODUCTORY RECORDS

       DO 25 I=1,10
  25   READ (15) WORD
       NUMPTS=0

C      READ POINTS

  30   READ (15) (XOUT(I),I=1,KGRAPH)
       IF(XOUT(1)-ENDS) 35,40,35
  35   NUMPTS=NUMPTS+1
       X(NUMPTS)=XOUT(1)
       U(NUMPTS)=XOUT(2)
       V(NUMPTS)=XOUT(3)
       W(NUMPTS)=XOUT(4)
       Y(NUMPTS)=XOUT(5)
```

67

```
      Z(NUMPTS)=XOUT(6)
      GO TO 30
   40 CONTINUE
C
C     CALL DRAW
C
      CALL DRAW(NUMPTS,X,U,MODCUR,0,LABEL,ITITLE,XSCL,YSCL,IUP,IRITE,
     CMODEX,MODEY,IW,IHI,IGR,LAST),I=1,12)
      READ(5,200)(ITITLE(I),I=1,12)
      CALL DRAW(NUMPTS,X,V,MODCUR,0,LABEL,ITITLE,XSCL,YSCL,IUP,IRITE,
     CMODEX,MODEY,IW,IHI,IGR,LAST),I=1,12)
      READ(5,200)(ITITLE(I),I=1,12)
      CALL DRAW(NUMPTS,X,W,MODCUR,0,LABEL,ITITLE,XSCL,YSCL,IUP,IRITE,
     CMODEX,MODEY,IW,IHI,IGR,LAST),I=1,12)
      READ(5,200)(ITITLE(I),I=1,12)
      CALL DRAW(NUMPTS,X,Y,MODCUR,0,LABEL,ITITLE,XSCL,YSCL,IUP,IRITE,
     CMODEX,MODEY,IW,IHI,IGR,LAST),I=1,12)
      READ(5,200)(ITITLE(I),I=1,12)
      CALL DRAW(NUMPTS,X,Z,MODCUR,0,LABEL,ITITLE,XSCL,YSCL,IUP,IRITE,
     CMODEX,MODEY,IW,IHI,IGR,LAST)
      NOCUR=NOCUR-1 55,45,50
      IF(NOCUR-1) 55,45,50
   45 MODCUR=3
      READ(15) WORD
      GO TO 20
   50 MODCUR=2
      READ(15) WORD
      GO TO 20
   55 NOPLOT=NOPLOT-1
      IF(NOPLOT) 60,60,5
   60 STOP
      END
C
C     DATA CARDS
C
      1
      1
U  VS TIME   U GUST INPUT
APCS INCL U AND DERIV U INPUTS     0   0     0     8     4     1
      0      0   0
W  VS TIME   U GUST INPUT
APCS INCL U AND DERIV U INPUTS
ZE VS TIME   U GUST INPUT
APCS INCL U AND DERIV U INPUTS
THRUST VS TIME U GUST INPUT
APCS INCL U AND DERIV U INPUTS
UGUST VS TIME
APCS INCL U AND DERIV U INPUTS
```

68

*** CSMP/360 SIMULATION DATA ***

```
FUNCTION TECURV=-2100.0,4.0,-1800.0,2.5,-1500.0,2.25,-1200.0, ...
2.18,-800.0,2.13,-400.0,2.08,-200.0,2.03,0.0,1.85,200.0,1.55, ...
400.0,1.77,600.0,0.1,15,800.0,0.1,1,1200.0,0.1,05,2300.0,0.1,0,3000.0, ...
1.0
PARAM A0=0.0242,A1=0.369,B0=66.489,B1=43.089,B2=9.7996,K=0.5923
INCON X10=0.0,X20=0.0,X30=0.0,X40=0.0,ZE0=0.0
CONSTANT KP=0.5,KUDOT=2.0
TIMER FINTIM=30.0,DELT=0.0500,OUTDEL=0.10,PRDEL=0.5
METHOD RKSFX
TITLE A-7F AIRCRAFT WITH APC/AFCS/ACL CLOSURES
PRINT ZE,THETAC,ELEV,ELEVP,NZBAR,PLA,THRUST,ERRCUM
PREPARE X1,X2,ZE,THRLST,UGUST

END

TIMER VARIABLES
DELT  = 5.0000E-02
DELMIN= 3.0000E-06
FINTIM= 3.0000E 01
PRDEL = 5.0000E-01
OUTDEL= 1.0000E-01
```

A-MATRIX

-0.054530	-32.159988	0.000000
-0.287000	0.0	218.000000
-0.000082	0.0	0.0
-0.007811	0.0	-0.390500

B-MATRIX

0.054530	0.001317	-0.732800
0.286950	0.000250	-14.714000
0.000082	0.000004	-2.184600
		-0.064330
		0.528870
		0.007811

C-MATRIX

-1.000000	218.000000	0.0
-0.528870	0.0	-0.286950
0.052334	0.0	0.000550

D-MATRIX

0.0	0.0	0.528870
-0.000250	0.286950	-0.052334
-0.000027	-0.000550	
	-14.714000	
	14.636800	

RR   A-7E AIRCRAFT WITH APC/AFCS/ACL CLOSURES   RKSFX   INTEGRATION

Column headers (rotated): TIME, 7E, THETAC, ELEV, ELEVP, NZBAR, PLA, THRUST, ERRCUM

PROBLEM DURATION 0.0   TO 3.0000E 01

VARIABLE	MINIMUM	TIME	MAXIMUM	TIME
X1	-4.4800E 00	1.5750E 01	2.4423E 00	2.1600E 01
X2	-5.3625E 00	1.4100E 01	2.4773E 00	1.9000E 01
ZF	-4.9204E 02	1.4900E 01	9.0174E 03	2.0000E 01
THRUST	-8.1744E 02	1.4800E 01	1.5541E 03	1.9500E 01
UGUST	-1.1338E 01	1.3700E 01	1.4372E 01	1.8650E 01

RMS VELOCITY ERROR= 4.0551

RMS GUST LEVEL: 5.0217
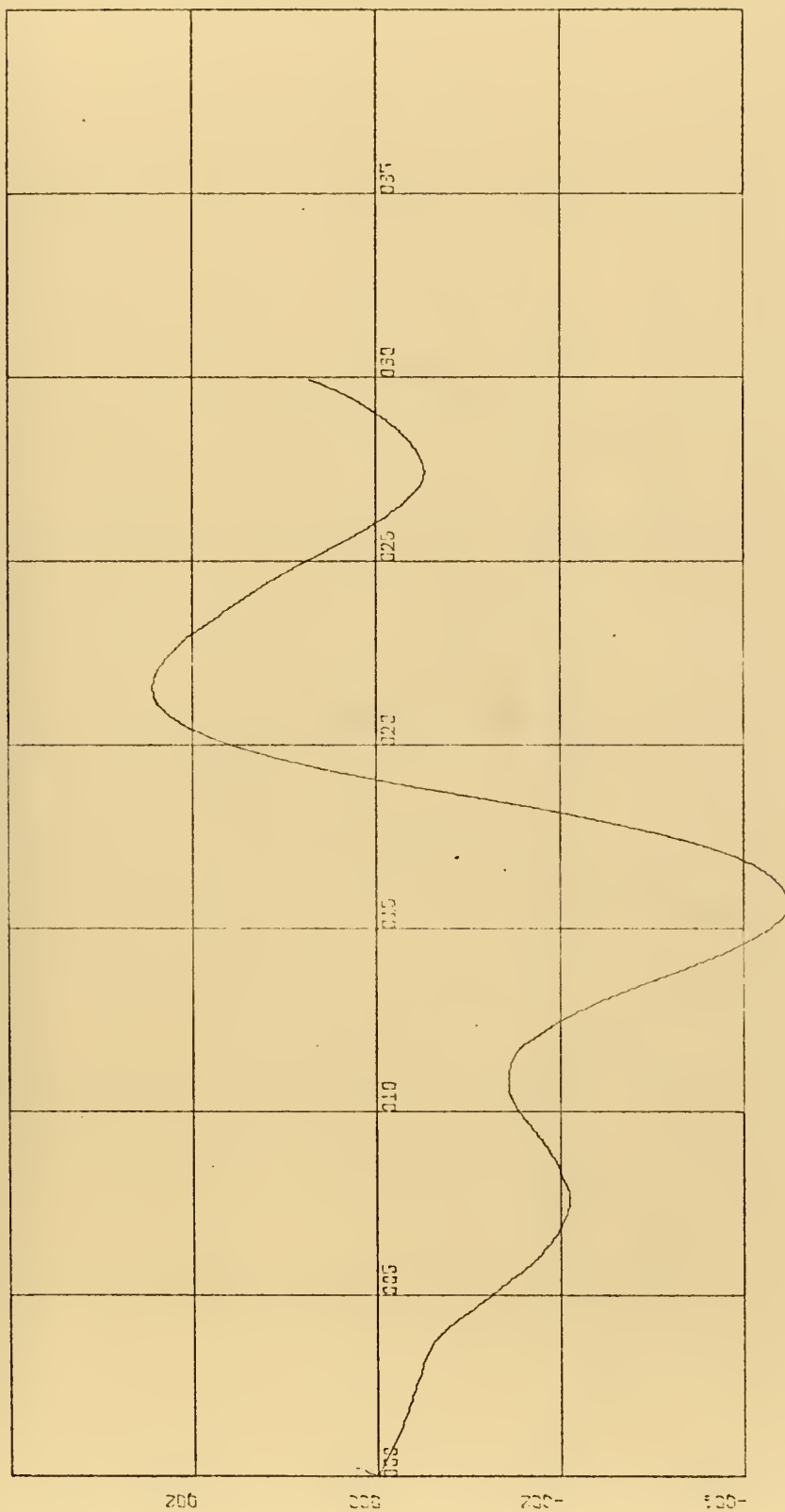
X-SCALE=5.00E+00 UNITS INCH.
Y-SCALE=2.00E+00 UNITS INCH.
U VS TIME   U GUST INPUT
APCS INCL U AND DERIV U INPUTS
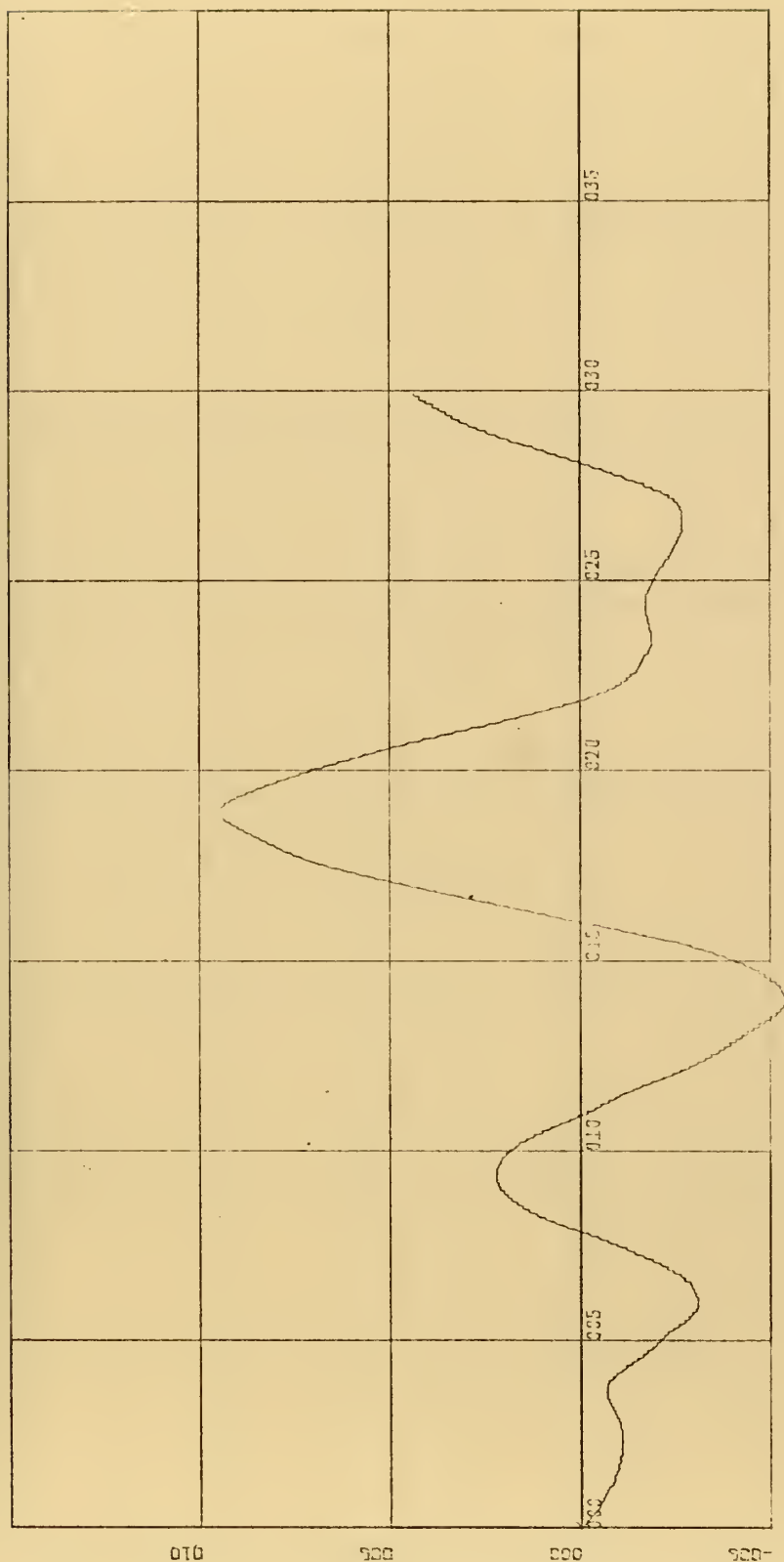
X-SCALE=5.00E+00 UNITS INCH.
Y-SCALE=5.00E+00 UNITS INCH.
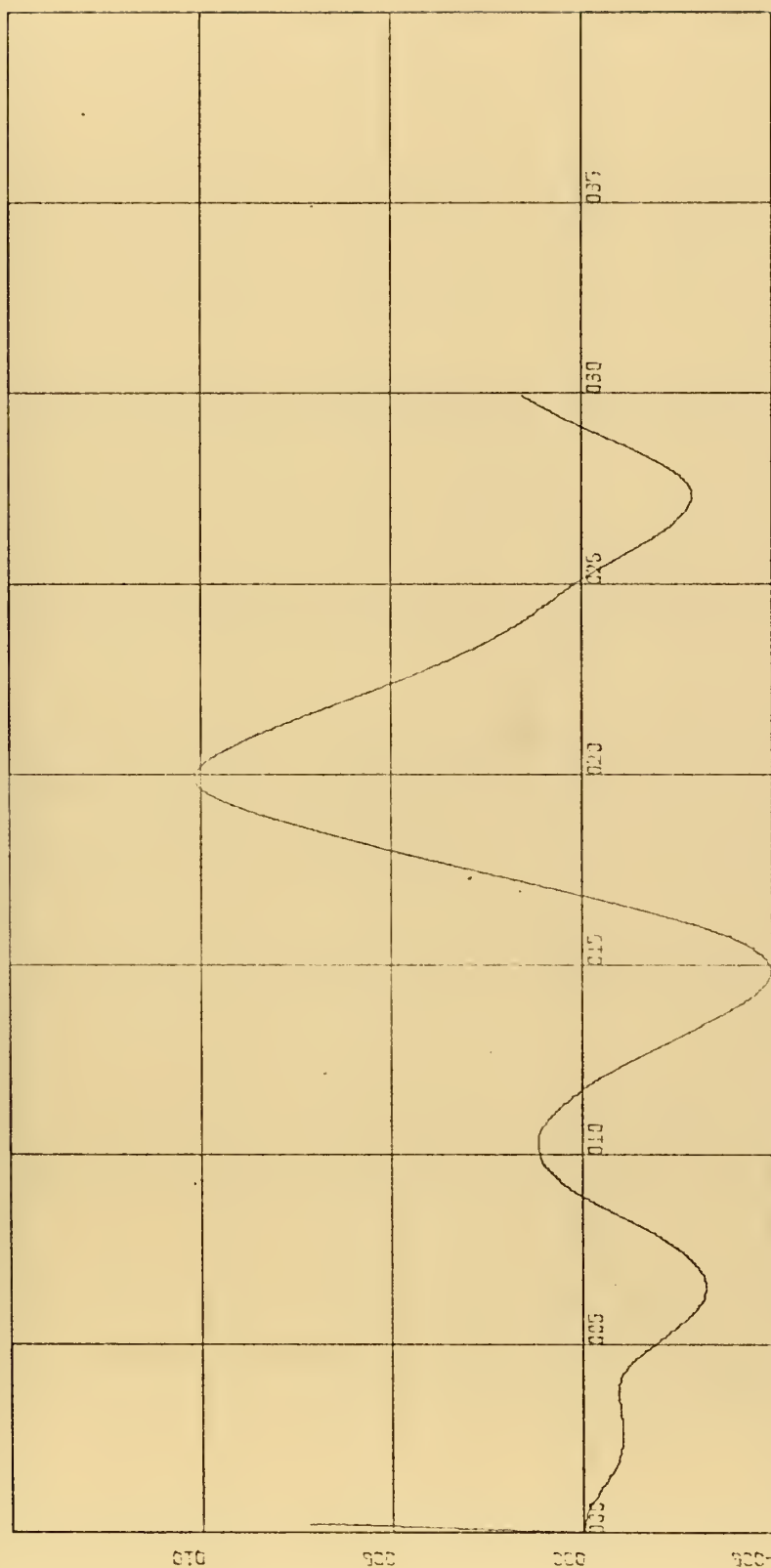W VS TIME   U GUST INPUT
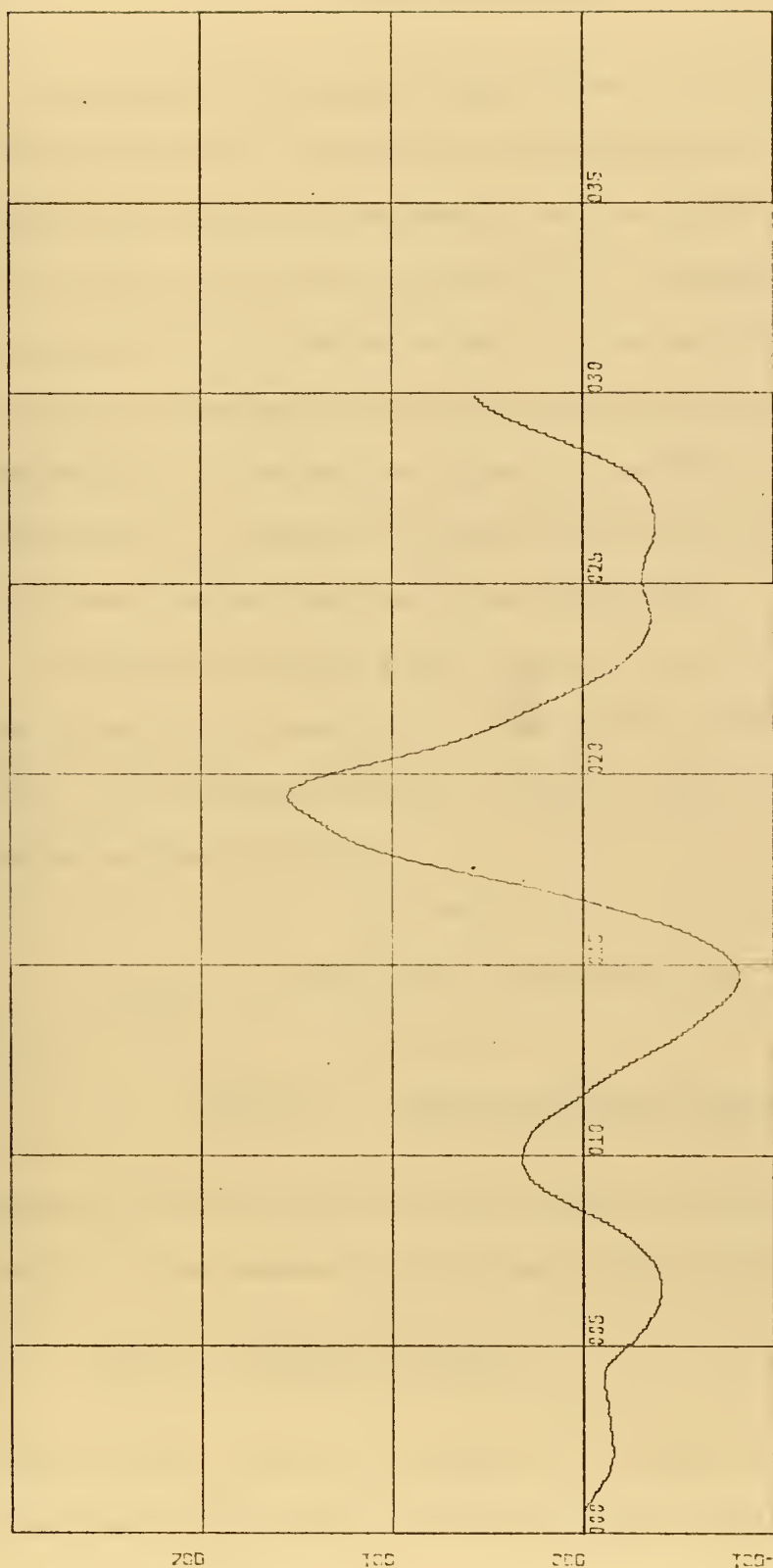APCS INCL U AND DERIV U INPUTS

73

74

X-SCALE=5.00E+00 UNITS INCH.
Y-SCALE=5.00E+00 UNITS INCH.
ZE VS TIME   U GUST INPUT
APCS INCL U AND DERIV U INPUTS

74

X-SCALE=5.00E+00 UNITS INCH.
Y-SCALE=1.00E+01 UNITS INCH.
UGUST VS TIME
APCS INCL U AND DERIV U INPUTS

X-SCALE=5.00E+00 UNITS INCH.
Y-SCALE=1.00E+03 UNITS INCH.
THRUST VS TIME U GUST INPUT
APCS INCL U AND DERIV U INPUTS

GUST MODEL ANALYSIS

To simulate a gust input for the CSMP simulation, a random number generator was used. The CSMP function RNDGEN has a uniform probability distribution function with possible values from 0.0 to 1.0. As the desired mean of the gust input was 0.0, a constant value of 0.5 was subtracted from the RNDGEN output. The output of the random number generator was passed through a CSMP second-order filter with a break frequency of 1.0 rad/sec and a damping coefficient of 0.707 and was multiplied by a constant to achieve an RMS value of 5.0. The following is a power spectral analysis of the gust model.

Denoting the RNDGEN output signal in the frequency domain as $X(j\omega)$, the filter Fourier Transform as $H(j\omega)$, and the resultant gust signal as $Y(j\omega)$, the relationship between $X(j\omega)$ and $Y(j\omega)$ is shown in Figure B.1. The output power spectral

$$X(j\omega) \longrightarrow \boxed{H(j\omega)} \longrightarrow Y(j\omega)$$

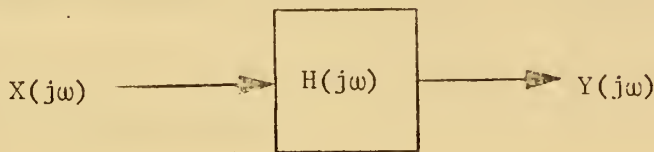FIGURE B.1 GUST MODEL BLOCK DIAGRAM

density is equal to the input power spectral density multiplied by the absolute value squared of the filter Fourier Transform:

$$\Phi_{yy}(j\omega) = \left| H(j\omega) \right|^2 \Phi_{xx}(j\omega) \tag{1}$$

The mean square value of the output, or average output power, can be determined by evaluating the autocorrelation function, $\varphi_{yy}(\tau)$, at $\tau = 0$:

$$\bar{y}^2 = \varphi_{yy}(0) = \frac{1}{2\pi} \int_{-\infty}^{\infty} \Phi_{yy}(j\omega)\ d\omega$$

(2)

$$= \frac{1}{2\pi} \int_{-\infty}^{\infty} \left| H(j\omega) \right|^2 \Phi_{xx}(j\omega)\ d\omega$$

$\bar{y}$ is defined as the RMS value of $y(t)$.

A typical time plot of $x(t)$ is shown in Figure B.2.
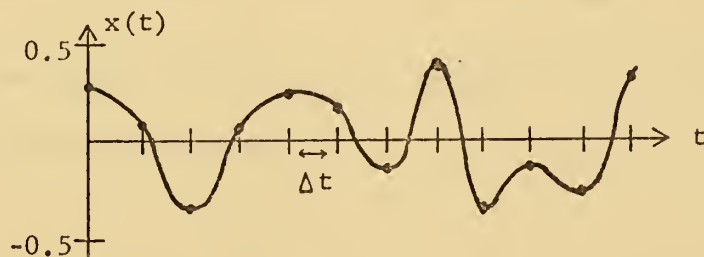
FIGURE B. 2   RNDGEN Output vs. Time

The random number generator output is a discrete value at each Δt.   The resultant curve through the points represents the fourth-order Runge-Kutta approximation of the function.   By approximating the curve by a series of steps, a rough approximation of the autocorrelation function, $\varphi_{xx}(\tau)$, was determined.

The autocorrelation function is defined by the equation,

$$\varphi_{xx}(\tau) = \int_{-\infty}^{\infty} x(t)\ x(t + \tau)\ dt$$

(3)

For the step series function utilized to approximate the RNDGEN output, each segment, Δt in length, is uncorrelated with every other segment; that is,

$$\varphi_{xx}(\tau) = 0 \qquad\qquad\qquad |\tau| > \Delta t \qquad (4)$$

78

To determine $\varphi_{xx}(\tau)$ subject to the restriction of Equation (4), $x(t)$ was depicted as in Figure B.3 [Ref. B.1]. By applying Equation (3)
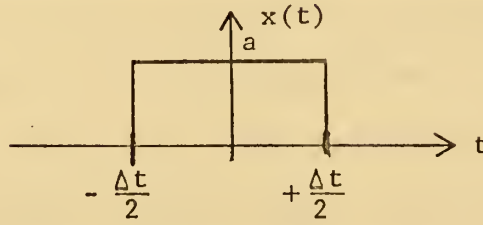
FIGURE B.3   Plot of x(t) to Determine $\varphi_{xx}(\tau)$

to Figure B.3 and requiring that $\varphi_{xx}(\tau)$ evaluated $\tau = 0$ be equal to the variance, $\varphi_{xx}(\tau)$ was determined.

$$\varphi_{xx}(\tau) = \sigma_x^2 \left(- \frac{|\tau|}{\Delta t} + 1 \right) \qquad\qquad |\tau| < \Delta t \qquad (5)$$

The power spectral density can be expressed

$$\Phi_{xx}(j\omega) = \int_{-\infty}^{\infty} \varphi_{xx}(\tau) e^{-j\omega\tau} \, d\tau \qquad\qquad (6)$$

By substituting Equation (5) into Equation (6) and noting that $\varphi_{xx}(\tau)$ is even function,

$$\Phi_{xx}(j\omega) = 2\sigma_x^2 (- \frac{1}{\Delta t} \tau + 1) \cos\omega\tau$$

$$= \frac{2\sigma^2}{\omega^2 \Delta t} \, (1 - \cos\omega\tau) \qquad\qquad (7)$$

By successively applying L'Hospital's Rule

$$\Phi_{xx}(0) = \sigma_x^2 \Delta t \qquad\qquad (8)$$

$\Phi_{xx}(j\omega)$ is periodic with a period equal to $2\pi/\Delta t$. For a small integration step size with the filter cutoff frequency of 1.0 rad/sec, $\Phi_{xx}(j\omega)$ is essentially flat in the frequency range of interest and can be considered a constant at the zero-frequency value shown in Equation (8). For a second-order filter with a break frequency of 1.0 rad/sec, the magnitude of the transfer function, $H(j\omega)$, squared has a -40 dB/decade slope for frequencies greater than 1.0 rad/sec. Based on the flat power spectral density at low frequencies and the filter cutoff frequency, the evaluation of Equation (2) was approximated by taking $\Phi_{xx}(j\omega)$ as a constant at its zero-frequency value. The resulting integral was

$$\varphi_{yy}(0) \;=\; \sigma_x^{\,2}\, t \cdot \frac{1}{2\pi} \int_{-\infty}^{\infty} \frac{\omega_n^{\,2}}{(j\omega)^2 + 2\zeta\omega_n(j\omega) + \omega_n^{\,2}}\, d\omega \tag{9}$$

and was of a form tabulated in Ref. B.2. Substituting for ω_n and ζ and evaluating,

$$\varphi_{yy}(0) \;=\; 0.354\sigma_x^{\,2} \cdot \Delta t = \overline{y}^{\,2}$$

At $\overline{y} = 5.0$ ft/sec and $\Delta t = 0.05$ sec,

$$\sigma_x = 37.6 \text{ ft/sec} \tag{10}$$

In actual simulation the value of σ_y was strongly dependent on the RNDGEN used in the simulation, varying from 1.7 to 3.1 with a mean of 2.4, all values falling below the predicted. RMS values of the input to the filter (the outputs of the RNDGEN's) were essentially constant at the predicted value. The underestimation of the value of σ_x required to achieve the desired value of σ_y was a direct result of the step approximation to the fourth-order integration. The reason for the large

variance in output RMS values was not determined but was suspected to be caused by the short run time. The length of each run was 30 seconds, or 3600 integration points. In the final model, σ_x was adjusted to obtain the desired value of 5.0 ft/sec for σ_y.

REFERENCES

[B.1]   Blakelock, J. H., Col, USAF, <u>Automatic Control of Aircraft and Missles</u>, Wiley, 1965.

[B.2]   Newton, G. C. Jr., Gould, L. A., and Kaiser, J. F., <u>Analytical Design of Linear Feedback Controls</u>, Wiley, 1957.

MULTIPLE LOOP CONTROL SYSTEM ANALYSIS

The multiple loop analysis technique described below is derived and demonstrated for a general case in Ref. C.1. The technique is a procedure for expressing specific closed loop transfer functions of a multiple loop system in terms of the elements of the open loop, feedforward and feedback matrices. The following is a two control input, three output example.

Consider the system

$$
\underset{[A]}{\begin{bmatrix} a_{11}, & a_{12}, & a_{13} \\ a_{21}, & a_{22}, & a_{23} \\ a_{31}, & a_{32}, & a_{33} \end{bmatrix}} \underset{\{X\}}{\begin{Bmatrix} X_1(s) \\ X_2(s) \\ X_3(s) \end{Bmatrix}} = \underset{[B]}{\begin{bmatrix} b_{11}, & b_{12} \\ b_{21}, & b_{22} \\ b_{31}, & b_{32} \end{bmatrix}} \underset{\{\delta\}}{\begin{Bmatrix} \delta_1(s) \\ \delta_2(s) \end{Bmatrix}} + \underset{[C]}{\begin{bmatrix} c_{11}, & c_{12} \\ c_{21}, & c_{22} \\ c_{31}, & c_{32} \end{bmatrix}} \underset{\{R\}}{\begin{Bmatrix} R_1(s) \\ R_2(s) \end{Bmatrix}} \qquad (1)
$$

Matrix elements are general and may contain operators. $[A]$ is the open loop system matrix, $\{X\}$ is a vector of variables, $\{\delta\}$ is a vector of control variables, and $\{R\}$ is a vector of external disturbances. The system will contain one feedforward and two feedback paths to drive the control variable δ_1, as depicted in Figure C.1.
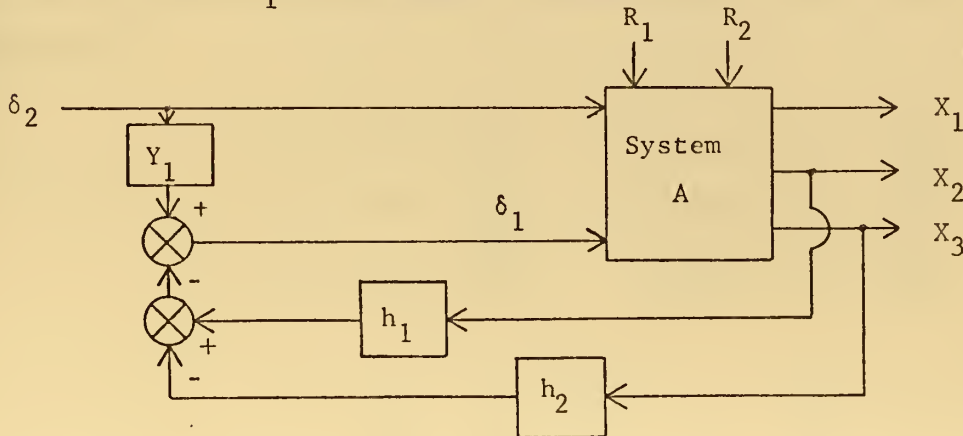

FIGURE C.1 Control System Block Diagram

The control equation is

$$\delta_1 = -h_1 X_2 - h_2 X_3 + Y_1 \delta_2 \tag{2}$$

The (s) notation has been dropped for simplicity. Substituting Equation (2) into (1) and rearranging

$$\begin{bmatrix} a_{11}, & a_{12}+h_1 b_{11}, & a_{13}+h_2 b_{11} \\ a_{21}, & a_{22}+h_1 b_{21}, & a_{23}+h_2 b_{21} \\ a_{31}, & a_{32}+h_1 b_{31}, & a_{33}+h_2 b_{31} \end{bmatrix} \begin{Bmatrix} X_1 \\ X_2 \\ X_3 \end{Bmatrix}$$

$$= \begin{bmatrix} b_{12}+Y_1 b_{11} \\ b_{22}+Y_1 b_{21} \\ b_{32}+Y_1 b_{31} \end{bmatrix} \delta_2 + \begin{bmatrix} c_{11}, & c_{12} \\ c_{21}, & c_{22} \\ c_{31}, & c_{32} \end{bmatrix} \begin{Bmatrix} R_1 \\ R_2 \end{Bmatrix} \tag{3}$$

Equation (3) is represented by the matrix notation

$$[A''] \{X\} = [B'] \{\delta_2\} + [C] \{R\}$$

where A'' denotes two loop closures and B' denotes one feedforward path. The closed loop system determinant can be expanded into a sum of four determinants

$$|A''| \equiv \Delta'' = \begin{vmatrix} a_{11}, & a_{12}, & a_{13} \\ a_{21}, & a_{22}, & a_{23} \\ a_{31}, & a_{32}, & a_{33} \end{vmatrix}_1 + \begin{vmatrix} a_{11}, & h_1 b_{11}, & a_{13} \\ a_{21}, & h_1 b_{21}, & a_{23} \\ a_{31}, & h_1 b_{31}, & a_{33} \end{vmatrix}_2$$

$$+ \begin{vmatrix} a_{11}, & a_{12}, & h_2 b_{11} \\ a_{21}, & a_{22}, & h_2 b_{21} \\ a_{31}, & a_{32}, & h_2 b_{31} \end{vmatrix}_3 + \begin{vmatrix} a_{11}, & h_1 b_{11}, & h_2 b_{11} \\ a_{21}, & h_1 b_{21}, & h_2 b_{21} \\ a_{31}, & h_1 b_{31}, & h_2 b_{31} \end{vmatrix}_4 \tag{4}$$

The determinant with a subscript of 1 is the open loop system determinant. Number 2 is the numerator of the open loop X_2/δ_1 transfer function multiplied by h_1. Number 3 is the numerator of the open loop X_3/δ_1 transfer function multiplied by h_2. Number 4 is identically equal to zero, as the second and third columns are proportional.

N_δ^x denotes the numerator of the open loop $X/\delta(s)$ transfer function. Using this notation, Equation (4) becomes

$$\Delta'' = \Delta + h_1 N_{\delta_1}^{x_2} + h_2 N_{\delta_1}^{x_3} \tag{5}$$

Equation (5) can be expanded for the general case to any order and number of closures as

$$\Delta^{n+m} = \Delta + \sum_{i=1}^{n} \sum_{j=1}^{m} h_{ij} N_{\delta_i}^{x_j} \tag{6}$$

h_{ij} represents the feedback transfer function from δ_i to x_j.

$N_{\delta_2}^{x_1} \Big]_{x_2, x_3, \delta_2 \to \delta_1}$ is defined as the closed loop numerator of the

X_1/δ_2 transfer function for the above loop closures.

From Equation (3)

$$N_{\delta_2}^{x_1} \Big]_{x_2, x_3, \delta_2 \to \delta_1} = \begin{vmatrix} b_{12} + Y_1 b_{11}, & a_{12} + h_1 b_{11}, & a_{13} + h_2 b_{11} \\ b_{22} + Y_1 b_{21}, & a_{22} + h_1 b_{21}, & a_{23} + h_2 b_{21} \\ b_{32} + Y_1 b_{31}, & a_{32} + h_1 b_{31}, & a_{33} + h_2 b_{31} \end{vmatrix} \tag{7}$$

Expanding Equation (7)

$$
N\begin{matrix} x_1 \\ \delta_2 \end{matrix}\bigg]_{x_2,\ x_3,\ \delta_2 \to \delta_1} = \begin{vmatrix} b_{12}, & a_{12}, & a_{13} \\ b_{22}, & a_{22}, & a_{23} \\ b_{32}, & a_{32}, & a_{33} \end{vmatrix} + \begin{vmatrix} Y_1 b_{11}, & a_{12}, & a_{13} \\ Y_1 b_{21}, & a_{22}, & a_{23} \\ Y_1 b_{31}, & a_{32}, & a_{33} \end{vmatrix}
$$

$$
+ \begin{vmatrix} b_{12}, & h_1 b_{11}, & a_{13} \\ b_{22}, & h_1 b_{21}, & a_{23} \\ b_{32}, & h_1 b_{31}, & a_{33} \end{vmatrix} + \begin{vmatrix} b_{12}, & a_{12}, & h_2 b_{11} \\ b_{22}, & a_{22}, & h_2 b_{21} \\ b_{32}, & a_{32}, & h_2 b_{31} \end{vmatrix} + 0 + 0 + 0 \qquad (8)
$$

Inspection of Equation (7) reveals that three determinants have dropped out. Equation (8) can be rewritten as

$$
N\begin{matrix} x_1 \\ \delta_2 \end{matrix}\bigg]_{x_2,\ x_3,\ \delta_2 \to \delta_1} = N\begin{matrix} x_1 \\ \delta_2 \end{matrix} + Y_1 N\begin{matrix} x_1 \\ \delta_1 \end{matrix} + h_1 N\begin{matrix} x_1 x_2 \\ \delta_2 \delta_1 \end{matrix} + h_2 N\begin{matrix} x_1 x_3 \\ \delta_2 \delta_1 \end{matrix} \qquad (9)
$$

where

$$
N\begin{matrix} x_1 x_2 \\ \delta_2 \delta_2 \end{matrix} \equiv \begin{vmatrix} b_{11}, & b_{12}, & a_{13} \\ b_{21}, & b_{22}, & a_{23} \\ b_{31}, & b_{32}, & a_{33} \end{vmatrix}
$$

Again, Equation (9) applies in general.

In the following case the output variable is X_2, one of the feedback variables.

$$
N\begin{matrix} x_2 \\ \delta_2 \end{matrix}\bigg]_{x_2,\ x_3,\ \delta_2 \to \delta_1} = \begin{vmatrix} a_{11}, & b_{12}+Y_1 b_{11}, & a_{13}+h_2 b_{11} \\ a_{21}, & b_{22}+Y_1 b_{21}, & a_{23}+h_2 b_{21} \\ a_{31}, & b_{32}+Y_1 b_{31}, & a_{33}+h_2 b_{31} \end{vmatrix}
$$

In the above notation

$$N_{\delta_2}^{x_2}\bigg]_{x_2,\; x_3,\; \delta_2 \to \delta_1} = N_{\delta_2}^{x_2} + Y_1 N_{\delta_1}^{x_2} + h_2 N_{\delta_2 \delta_1}^{x_2 x_3} \tag{10}$$

In Equation (10) another crossproduct was lost. This was a special case, but the notation of Equation (9) applies, noting that the lost term would have been $h_1 N_{\delta_2 \delta_1}^{x_2 x_2}$. A numerator of this form makes no sense and is defined as identically zero.

The following is a numerator of a transfer function of an output variable due to an external disturbance.

$$N_{r_1}^{x_1}\bigg]_{x_2,\; x_3,\; \delta_2 \to \delta_1} = \begin{vmatrix} c_{11}, & a_{12}+h_1 b_{11}, & a_{13}+h_2 b_{11} \\ c_{21}, & a_{22}+h_1 b_{21}, & a_{23}+h_2 b_{21} \\ c_{31}, & a_{32}+h_1 b_{31}, & a_{33}+h_2 b_{31} \end{vmatrix}$$

$$= N_{r_1}^{x_1} + h_1 N_{r_1 \delta_1}^{x_1 x_2} + h_2 N_{r_1 \delta_1}^{x_1 x_3} \tag{11}$$

Equation (11) is similar to Equation (9), but the feedforward term is missing. The notation of equation (11) applies to any external input for which there is no feedforward term, either for another control variable or for an actual external disturbance, as illustrated.

It should be noted that $N_{\delta_1 \delta_2}^{x_2 x_3}$ and $N_{\delta_2 \delta_1}^{x_3 x_2}$ denote the same determinant; i.e., rows are not interchanged. The latter notation would arise if $N_{\delta_2}^{x_3}\bigg]_{x_2,\; x_3,\; \delta_2 \to \delta_1}$ were formed.

REFERENCE

[C.1] Air Force Flight Dynamics Laboratory Report TDR-62-1014, <u>Analysis of Multiloop Vehicular Control Systems</u>, by D. T. McRuer, I. L. Ashkenas, and H. R. Pass, March 1964.

INITIAL DISTRIBUTION LIST

No. Copies

1. Defense Documentation Center   2
    Cameron Station
    Alexandria, Virginia   22314

2. Library, Code 0212   2
    Naval Postgraduate School
    Monterey, California   93940

3. Chairman, Department of Aeronautics   1
    Naval Postgraduate School
    Monterey, California   93940

4. Professor R. A. Hess, Code 57He   1
    Department of Aeronautics
    Naval Postgraduate School
    Monterey, California   93940

5. LT D. H. Finney, USN   1
    451 Dela Vina Avenue, Apt. 412
    Monterey, California   93940

6. Commander   1
    Naval Air Systems Command (PMA-235)
    Navy Department
    Washington, D. C.   20360

7. Professor G. J. Thaler, Code 52Tr   1
    Department of Electrical Engineering
    Naval Postgraduate School
    Monterey, California   93940

DOCUMENT CONTROL DATA - R & D

(Security classification of title, body of abstract and indexing annotation must be entered when the overall report is classified)

1. ORIGINATING ACTIVITY (Corporate author)	2a. REPORT SECURITY CLASSIFICATION
Naval Postgraduate School Monterey, California 93940	Unclassified
	2b. GROUP

3. REPORT TITLE

A REVISED DESIGN CONCEPT FOR THE A-7E APPROACH POWER COMPENSATOR SYSTEM

4. DESCRIPTIVE NOTES *(Type of report and inclusive dates)*
Master's Thesis; March 1973

5. AUTHOR(S) *(First name, middle initial, last name)*

DAVID H. FINNEY

6. REPORT DATE	7a. TOTAL NO. OF PAGES	7b. NO. OF REFS
March 1973	91	12

8a. CONTRACT OR GRANT NO.	9a. ORIGINATOR'S REPORT NUMBER(S)
b. PROJECT NO.	
c.	9b. OTHER REPORT NO(S) *(Any other numbers that may be assigned this report)*
d.	

10. DISTRIBUTION STATEMENT

Approved for public release; distribution unlimited.

11. SUPPLEMENTARY NOTES	12. SPONSORING MILITARY ACTIVITY
	Naval Postgraduate School Monterey, California 93940

13. ABSTRACT

The present concept of automatic throttle control, as employed in Navy carrier-based aircraft, was investigated. The aircraft chosen for study was the A-7E. The powerplant was the TF41-A-2, a turbofan engine with a relatively slow throttle response in the approach power range.

The effects of additional inputs to the approach power compensator were evaluated. It was shown that a considerable increase in performance could be achieved through the incorporation of longitudinal feedback. In addition, the limitations imposed on performance by large engine lags were found to be much less severe for systems with longitudinal feedback. The modifications suggested require a redesign of the approach power compensator system currently in use by the Navy.

DD FORM 1473 (PAGE 1)
1 NOV 65

S/N 0101-807-6811

14. KEY WORDS	LINK A		LINK B		LINK C	
	ROLE	WT	ROLE	WT	ROLE	WT
APPROACH POWER COMPENSATOR SYSTEM						
AUTOMATIC THROTTLE CONTROL						
AUTOMATIC POWER CONTROL						
AIRSPEED CONTROL						
AUTOMATIC CARRIER LANDING						
A-7E AIRCRAFT						